Understanding the multi-phase structure and physical conditions of the ISM

A dominant reservoir of CO-dark molecular gas in 30 Doradus

Mélanie Chevance

Heidelberg University

SOFIA tele-talk – 16 September 2020

Collaborators:

Suzanne Madden
Christian Fisher
William Vacca
Vianney Lebouteiller
Nick Abel
Dario Fadda
Frederic Galliano
Norbert Geis
Christof Iserlohe
Alfred Krabbe
Diederik Kruijssen
Albrecht Poglitsch
Fiorella Polles
Hans Zinnecker

Galaxy formation in a cosmological context

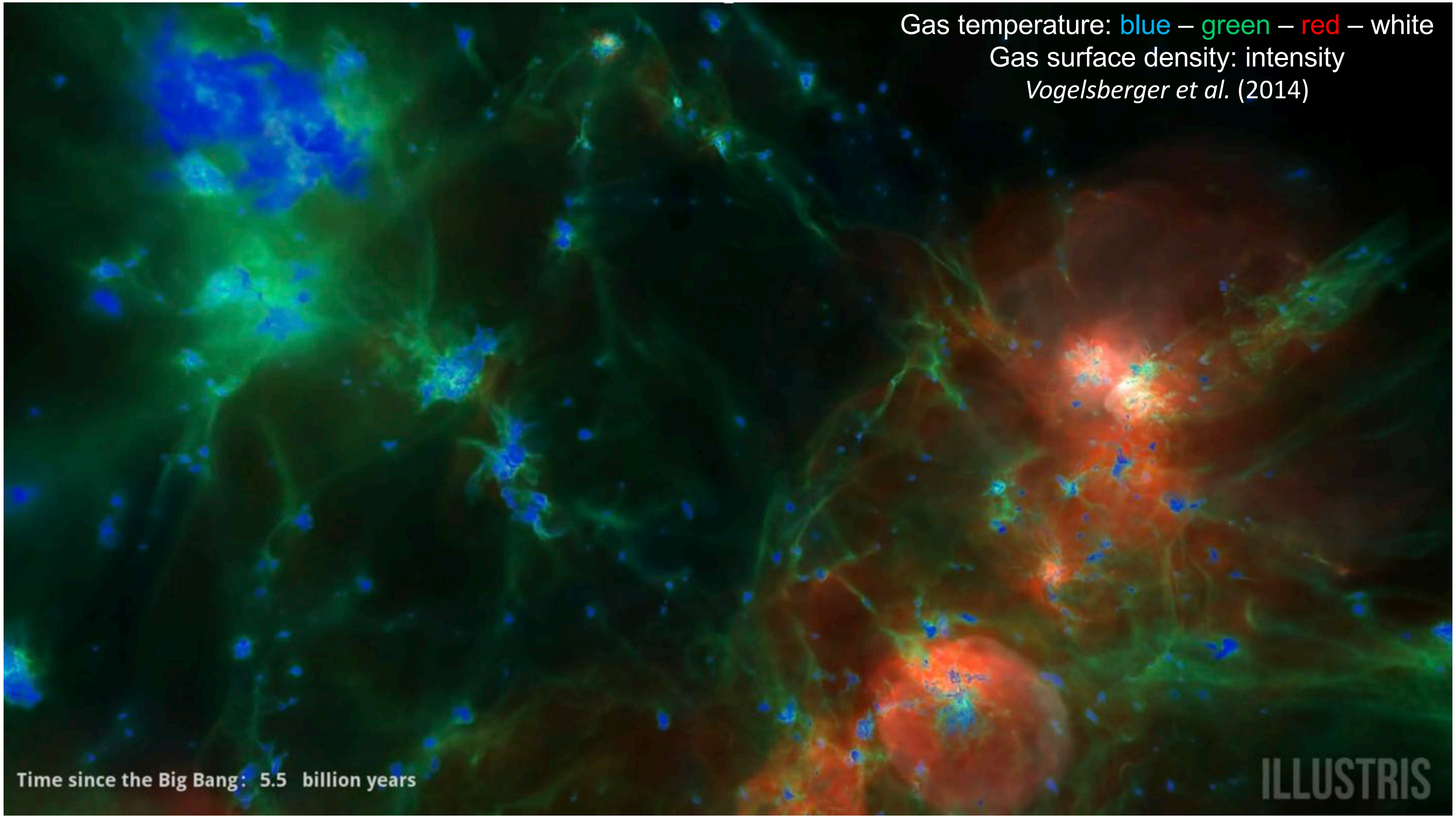

Star formation and feedback in galaxy simulations

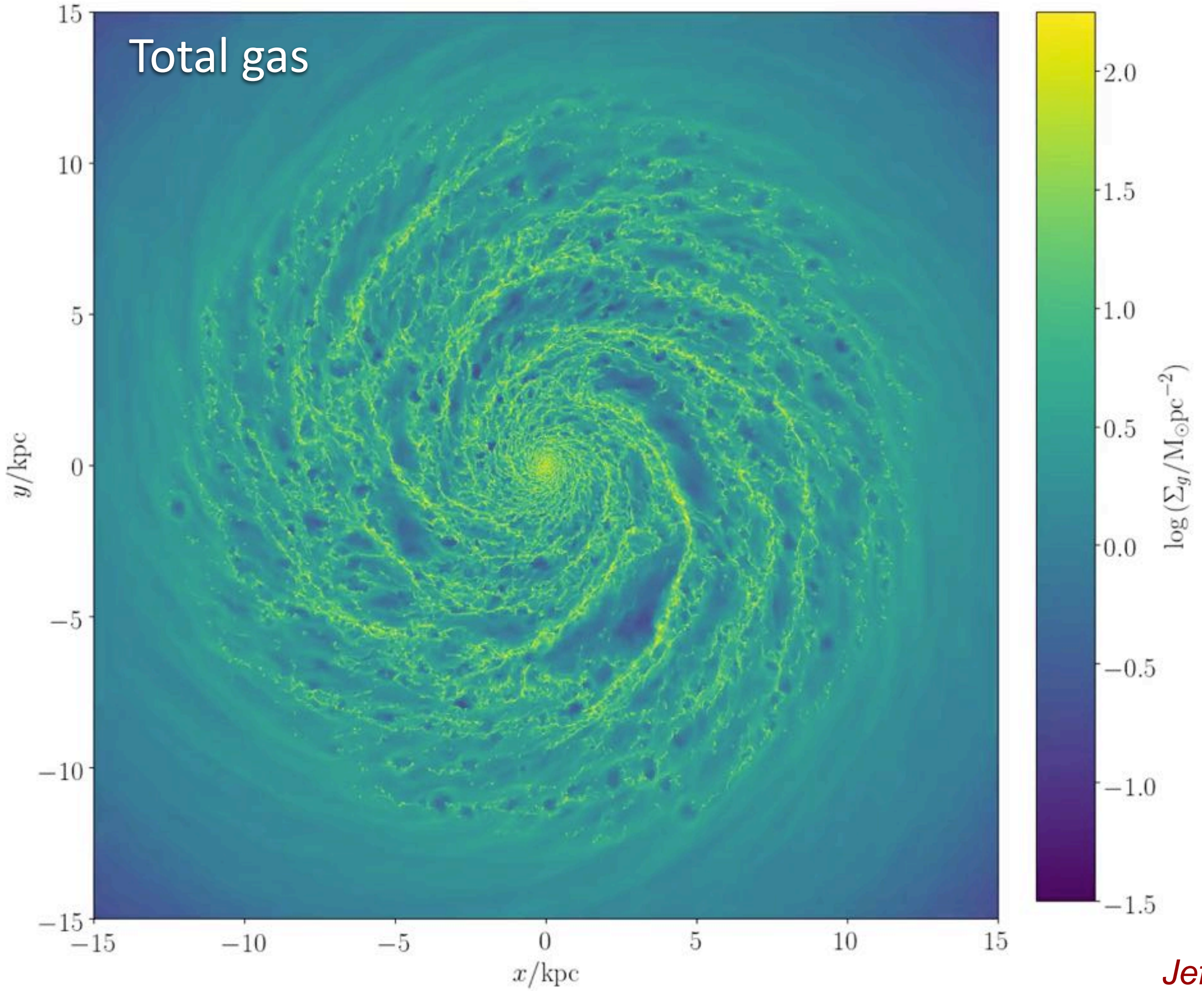

Jeffreson et al. (2020)

Uncertainties on the physics of star formation and feedback

Different criteria for star-forming gas

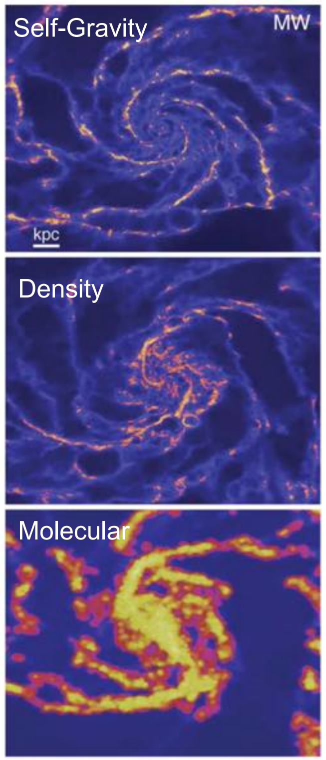

Hopkins et al. 2013

Gas surface density:
blue – red – yellow

Different feedback prescriptions

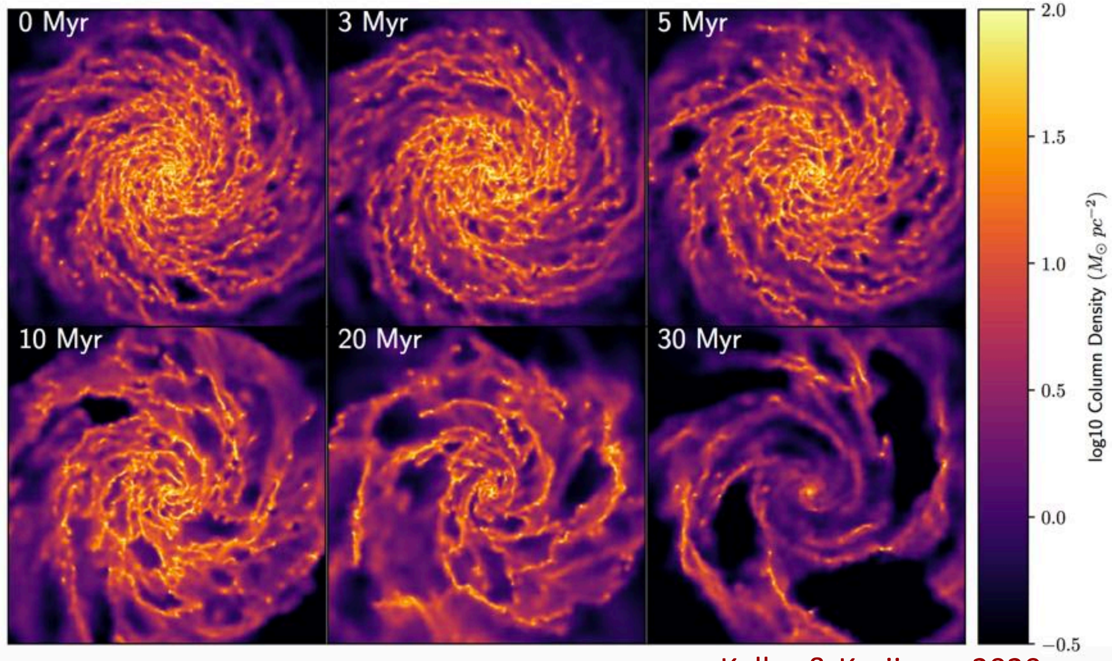

Keller & Kruijssen 2020

Understanding the multi-phase structure and physical conditions of the ISM

- **Multi-wavelength** observations,
- In a **variety of environments**,
- At **high spatial resolution**

Understanding the multi-phase structure and physical conditions of the ISM

- **Multi-wavelength** observations, → [OI], [CII], [OIII], [NIII]
- In a **variety of environments**,
- At **high spatial resolution**

Understanding the multi-phase structure and physical conditions of the ISM

- **Multi-wavelength** observations, → [OI], [CII], [OIII], [NIII]
- In a **variety of environments**, → Range of metallicities, densities, SF activity
- At **high spatial resolution**

Understanding the multi-phase structure and physical conditions of the ISM

- **Multi-wavelength** observations, → [OI], [CII], [OIII], [NIII]
- In a **variety of environments**, → Range of metallicities, densities, SF activity
- At **high spatial resolution** → Nearby galaxies

Diagnostic of various phases in the ISM

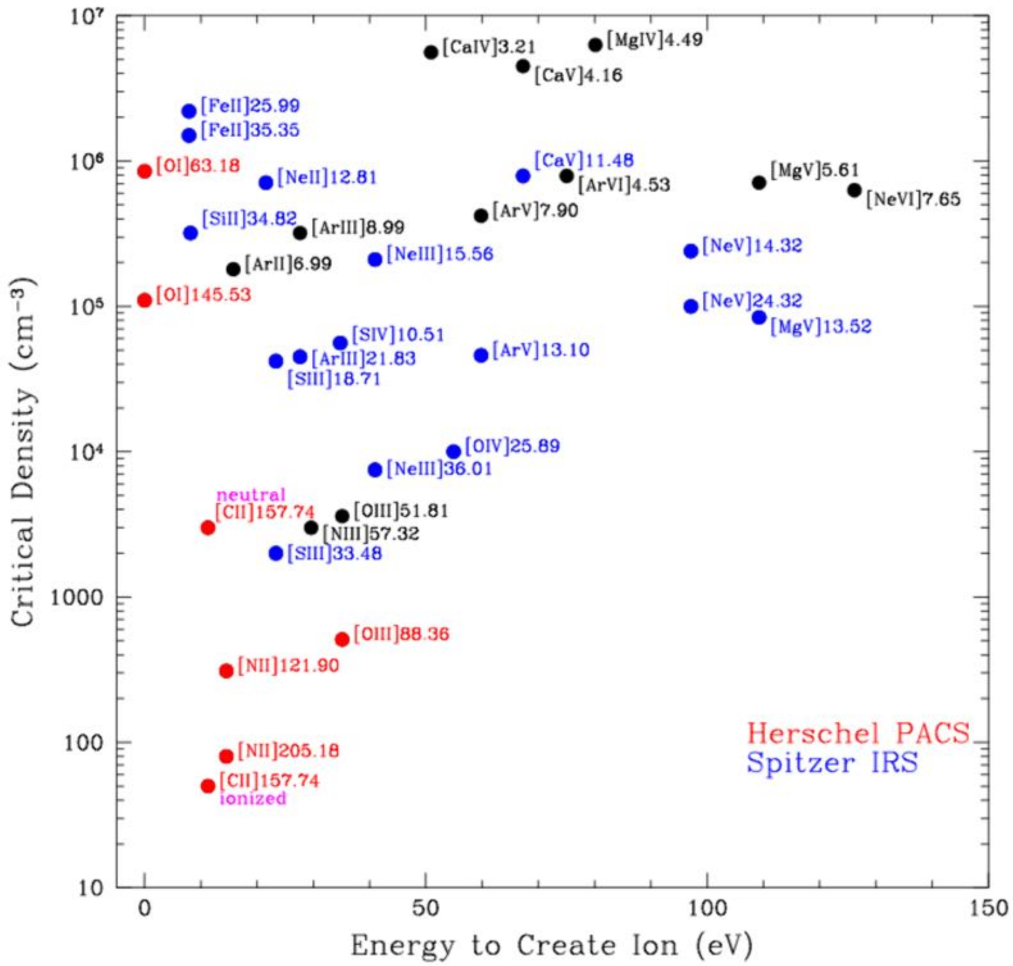

Kennicutt et al. 2011

Diagnostic of various phases in the ISM

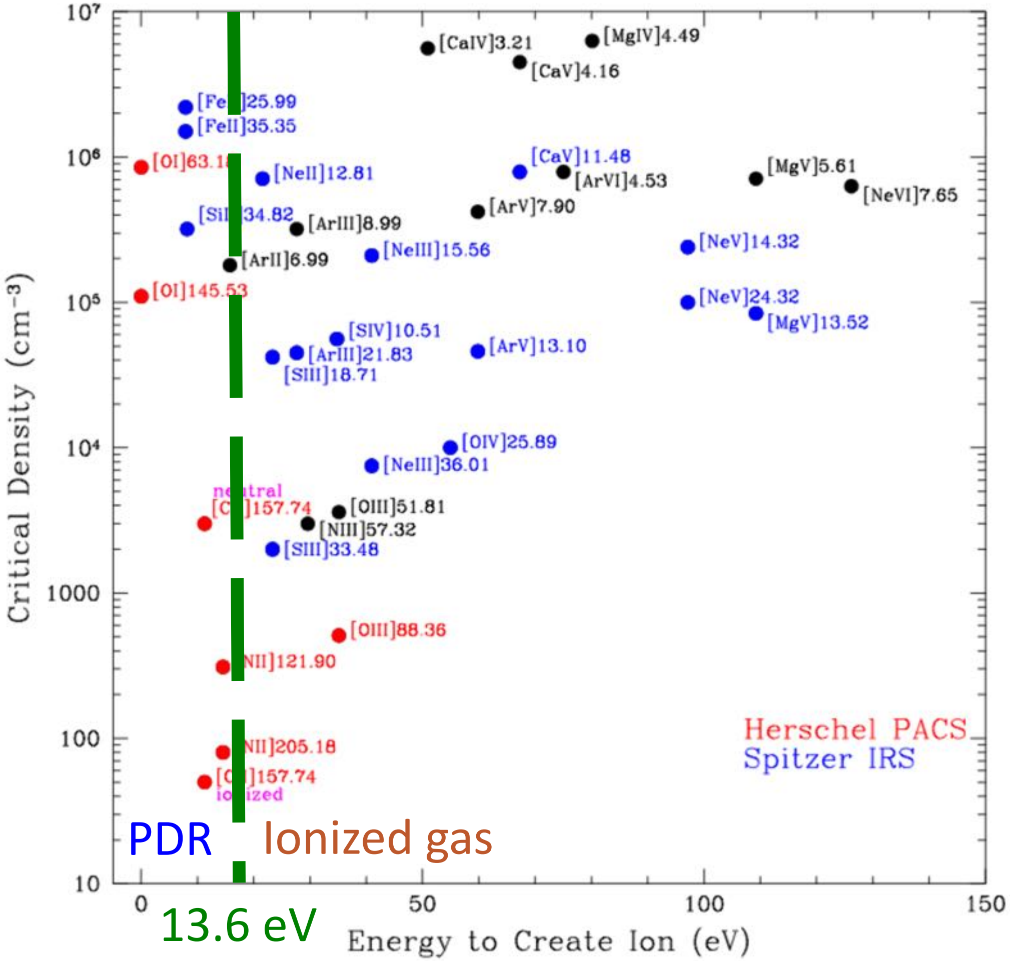

Kennicutt et al. 2011

Diagnostic of various phases in the ISM

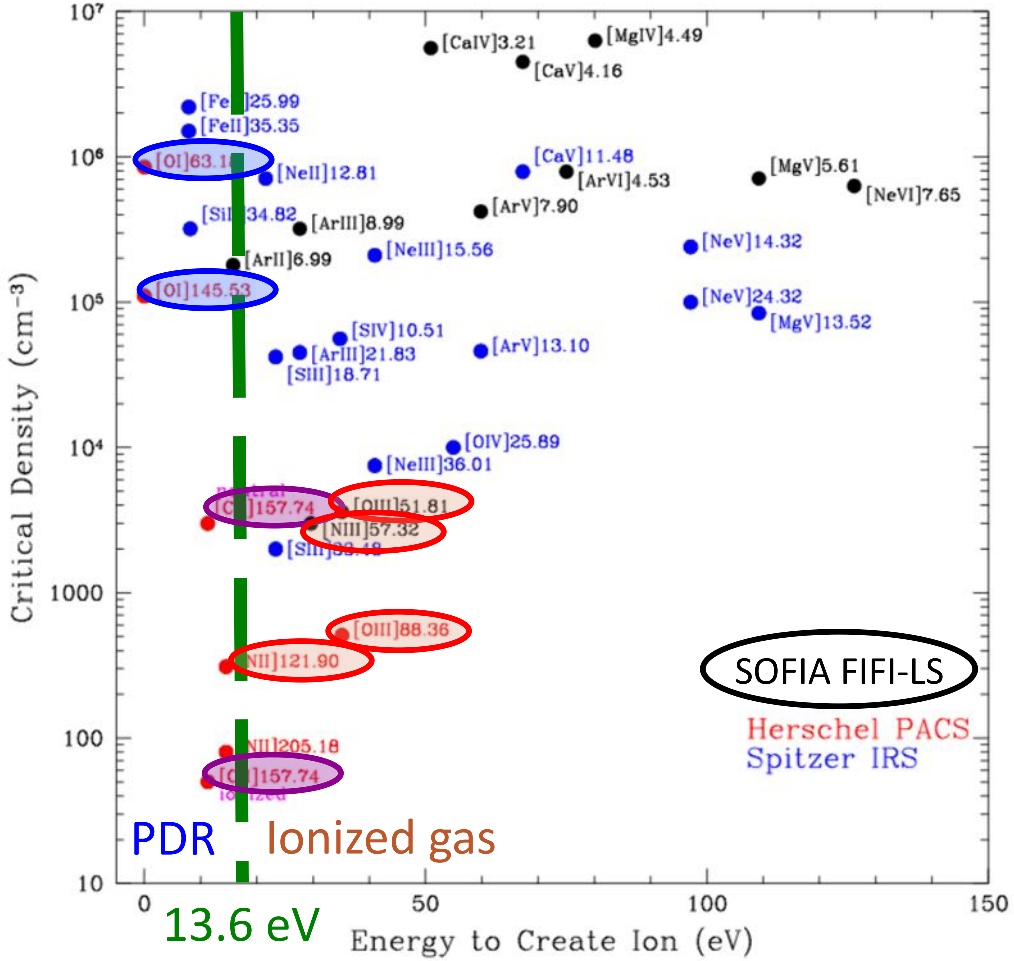

Kennicutt et al. 2011

Structure of the ISM

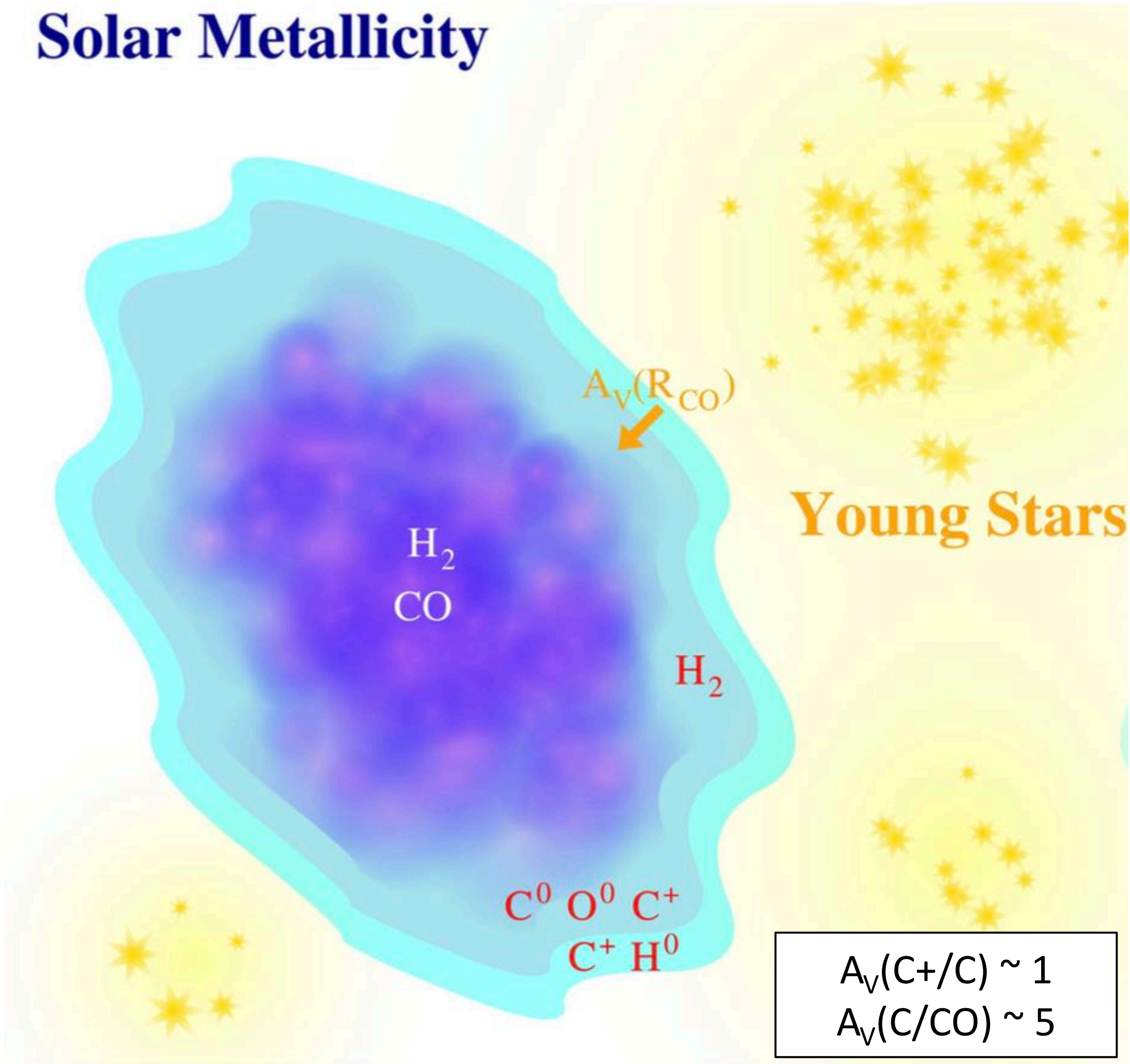

Madden et al. 2020

Structure of the ISM

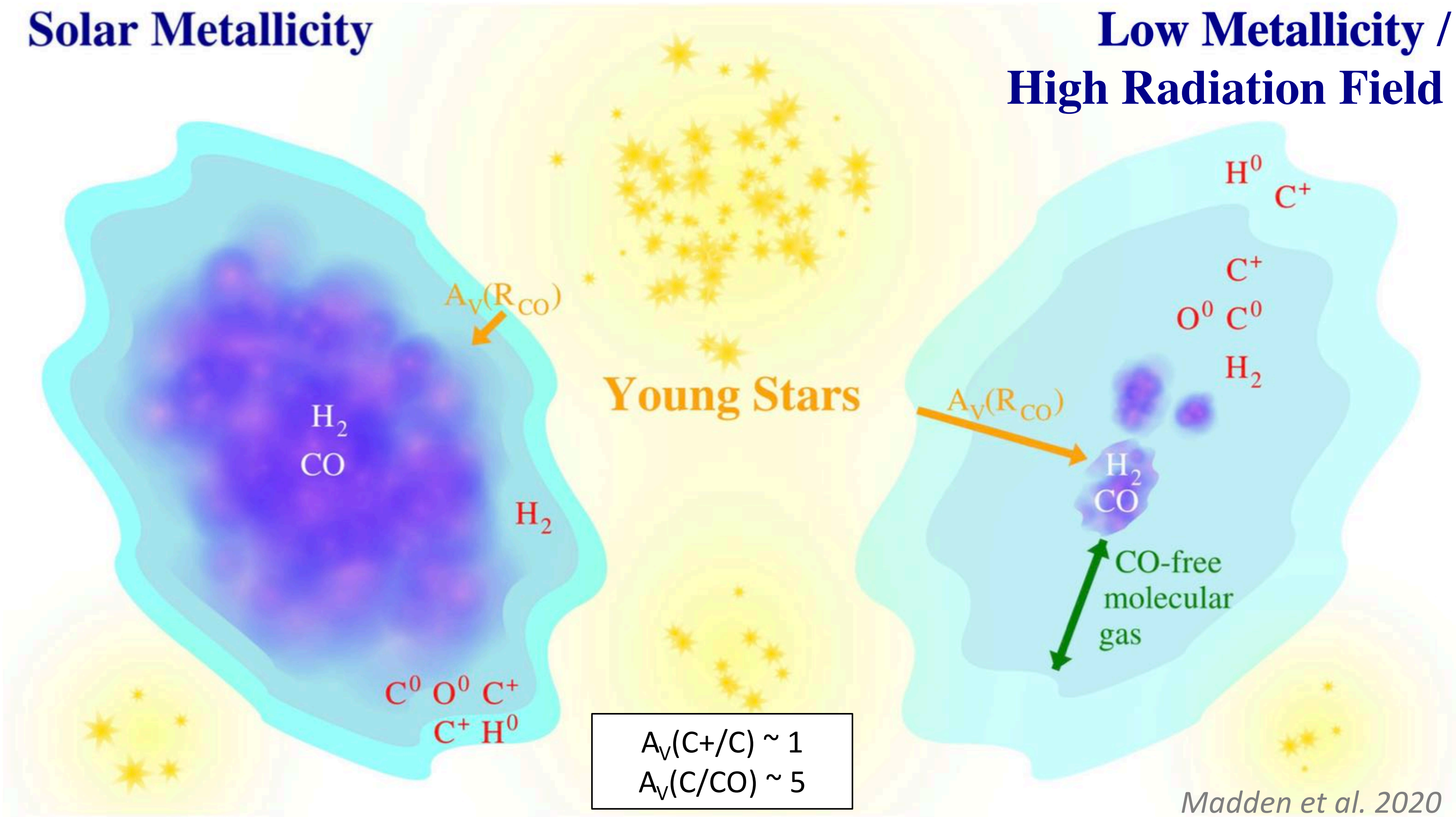

A_V(C+/C) ~ 1
A_V(C/CO) ~ 5

Madden et al. 2020

Low metallicity nearby galaxies

LMC 30 Dor
$Z = 1/2\ Z_{\odot}$
$D = 50$ kpc

IC10
$Z = 1/3\ Z_{\odot}$
$D = 700$ kpc

NGC1569
$Z = 1/4\ Z_{\odot}$
$D = 3.36$ Mpc

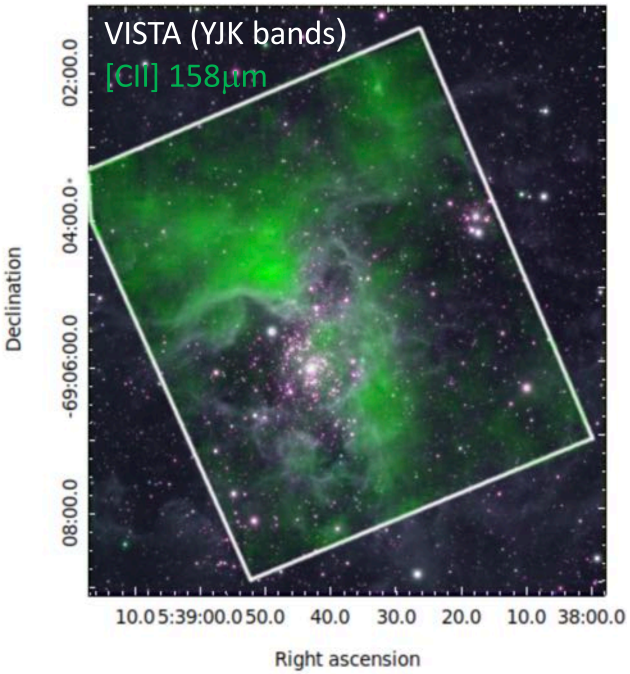

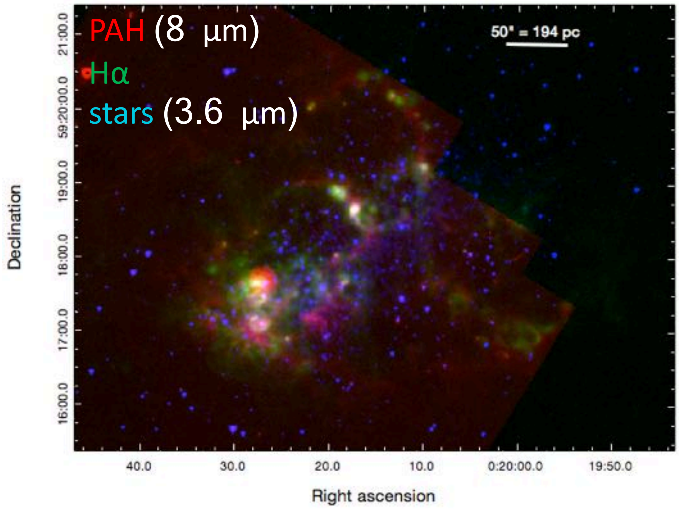

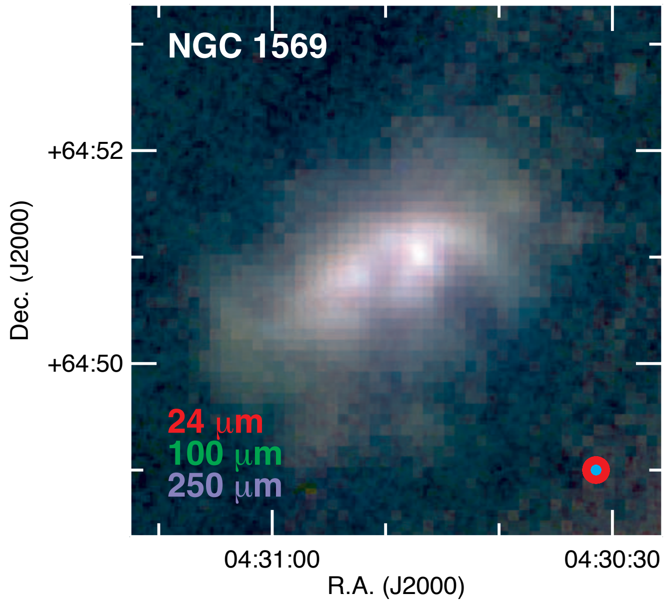

SOFIA/FIFI-LS data: 30Dor

Chevance et al. 2020b

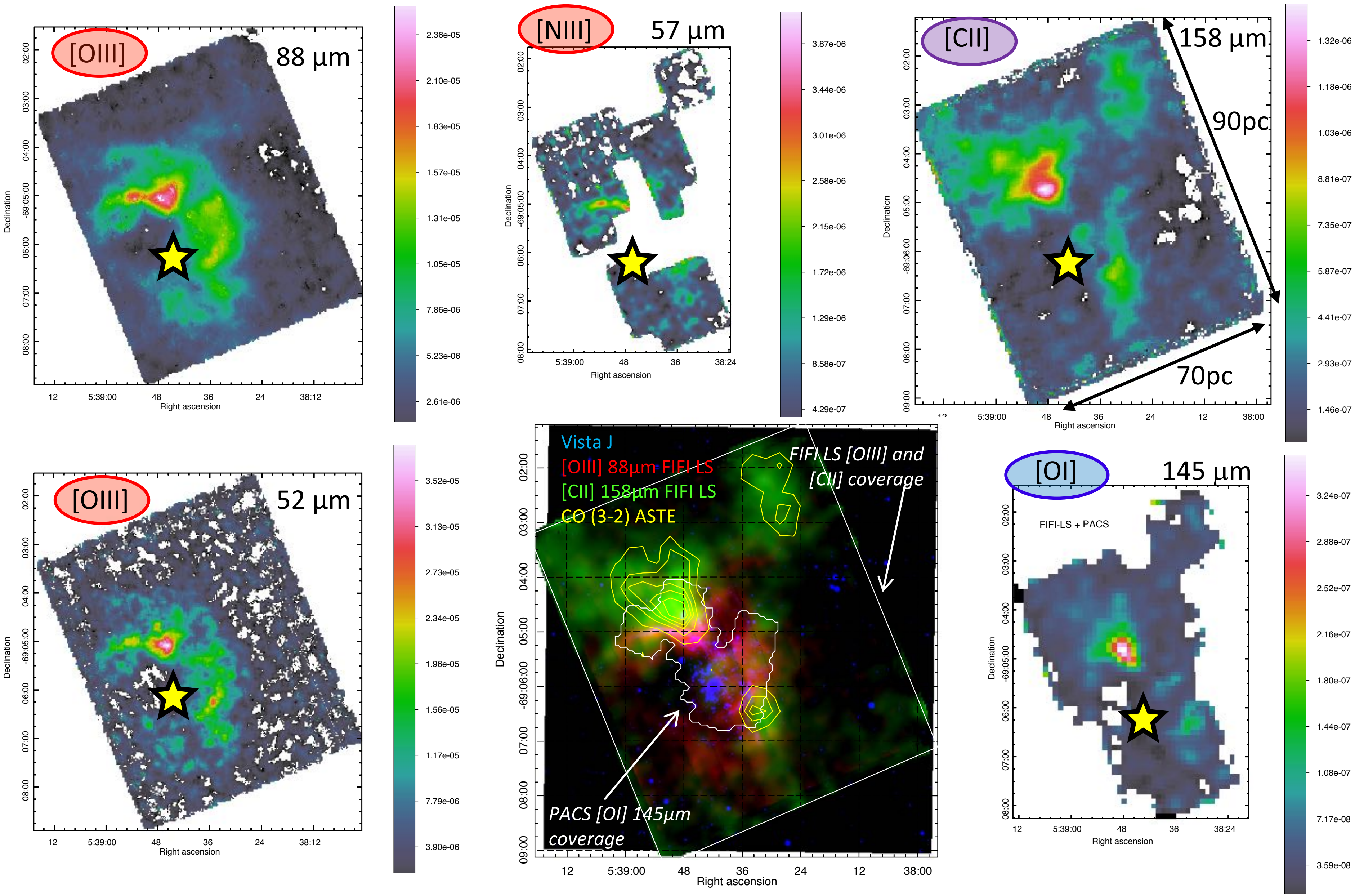

Spitzer, Herschel & SOFIA data: IC10

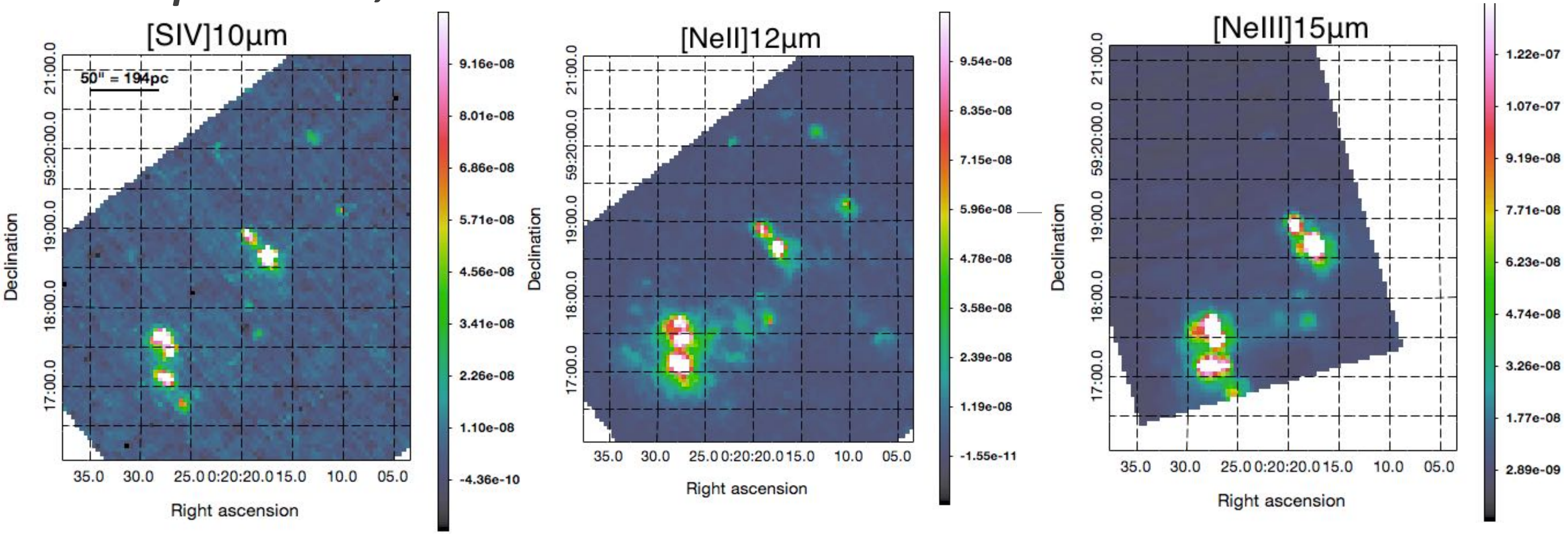

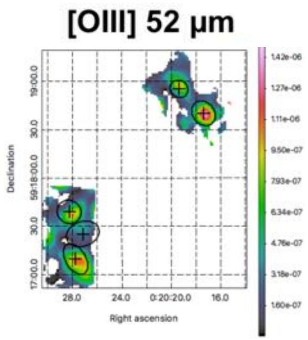

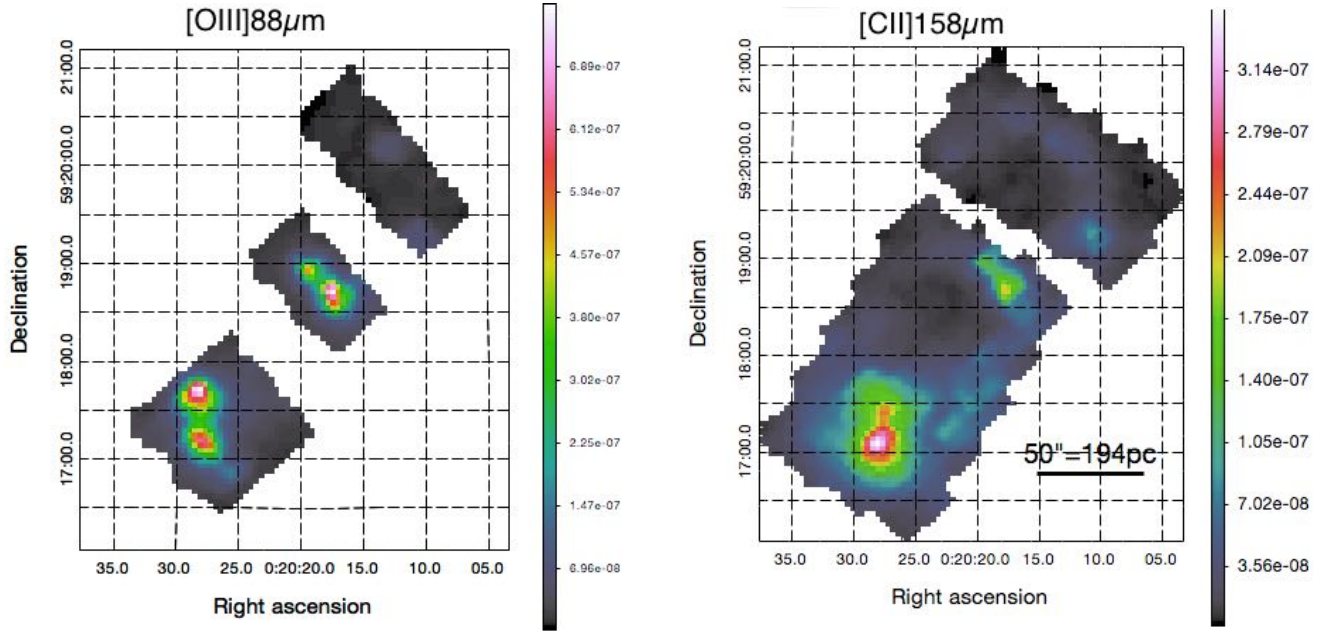

Polles et al. 2019
Polles et al. in prep.

SOFIA/FIFI-LS data: NGC 1569

FIFI-LS [OIII] 52μm (smoothed)

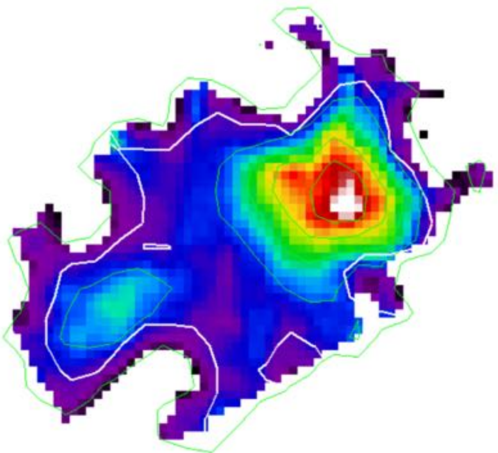

PACS [OIII] 88μm

Contours: [OIII] 52μm

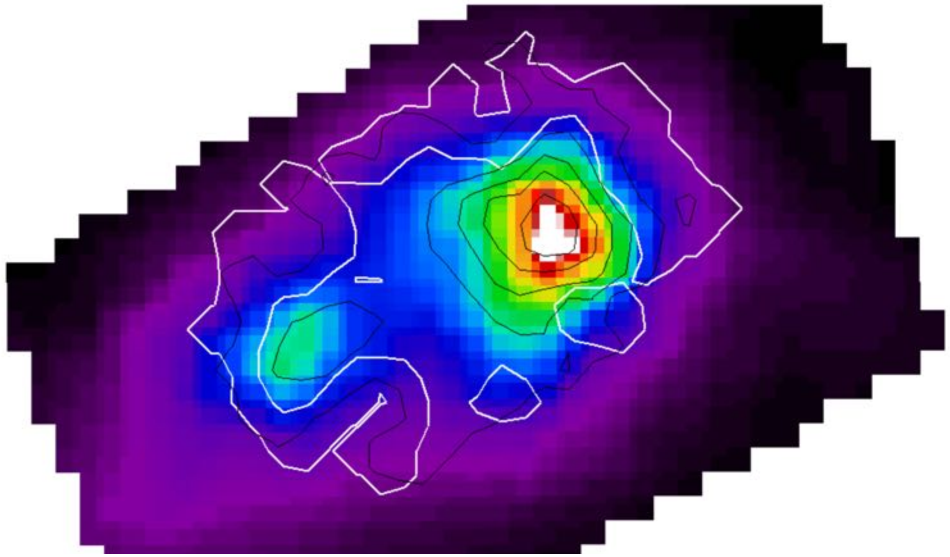

Maps: C. Fisher

Empirical diagnostics:
Electron density in the ionised gas

[OIII] 52μm / [OIII] 88μm

30 Dor

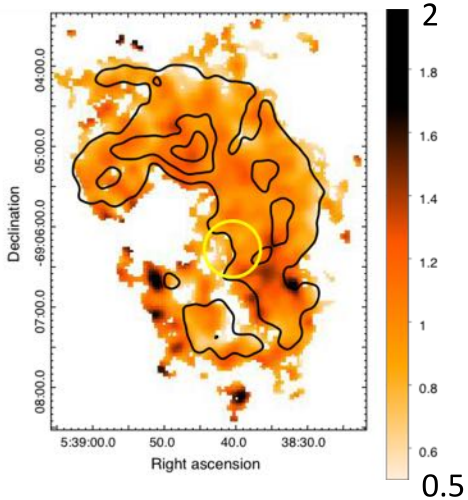

NGC 1569

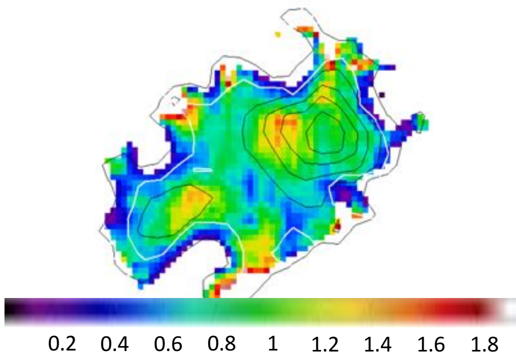

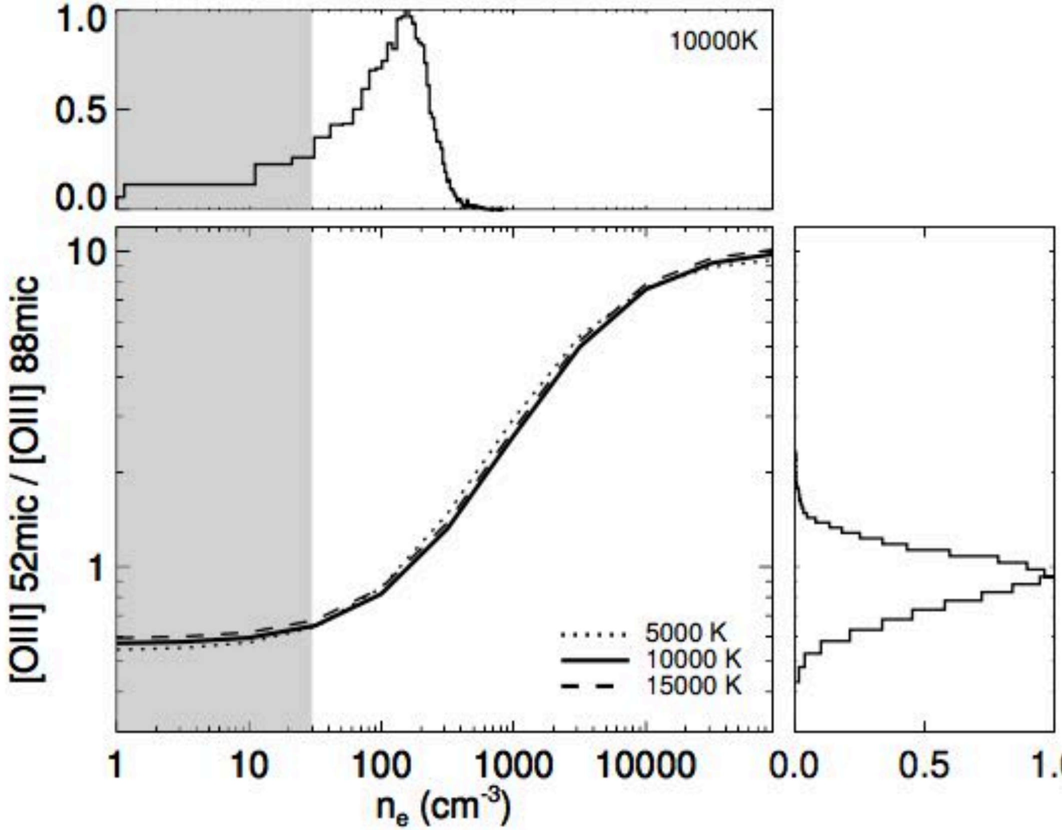

Chevance et al. 2020b

Mélanie Chevance

Empirical diagnostics:
Electron density in the ionised gas

[OIII] 52μm / [OIII] 88μm

30 Dor

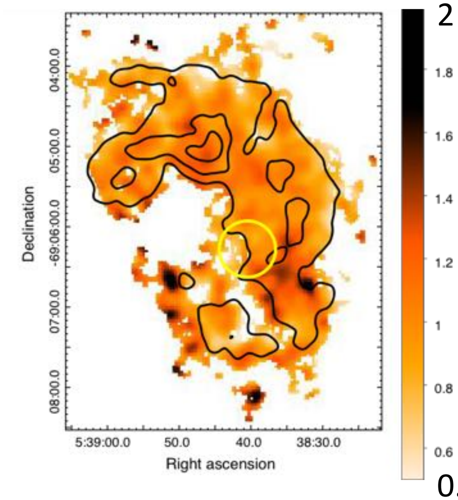

NGC 1569

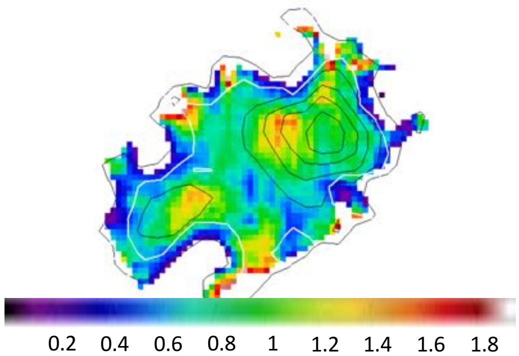

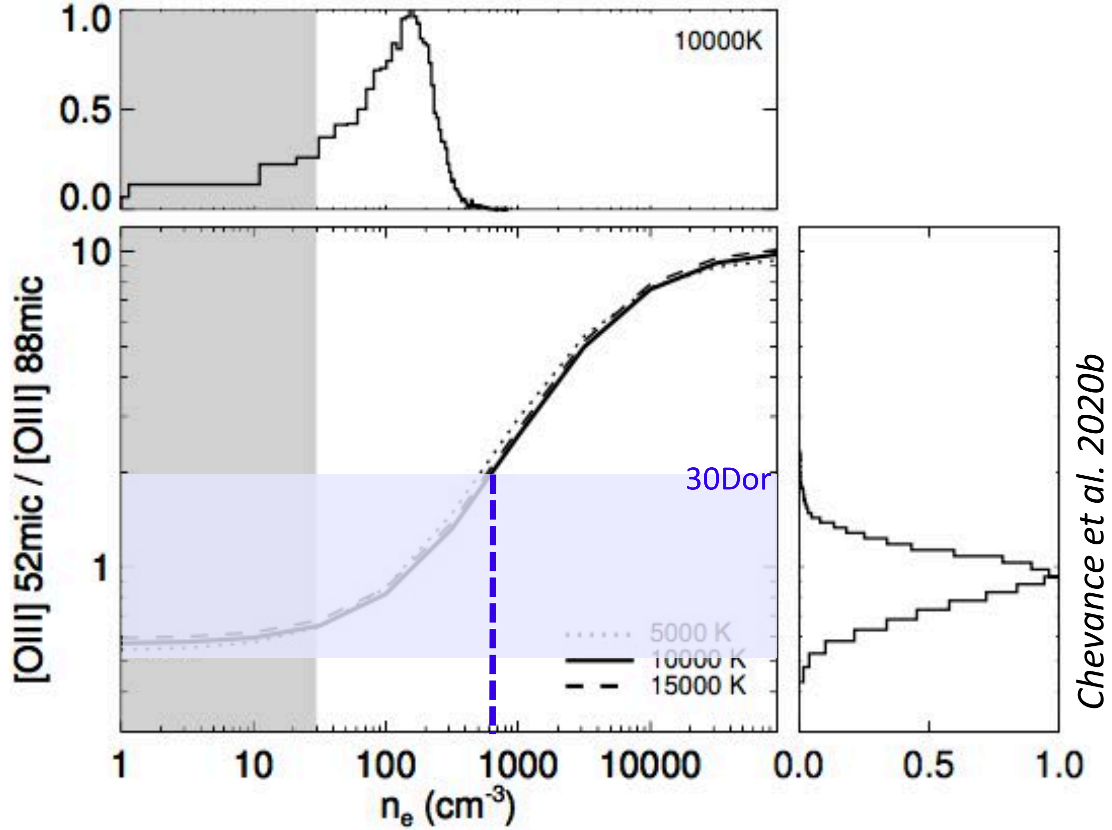

- 30Dor: electron density in the ionised gas < 600 cm^{-3}

Empirical diagnostics:
Electron density in the ionised gas

[OIII] 52μm / [OIII] 88μm

30 Dor

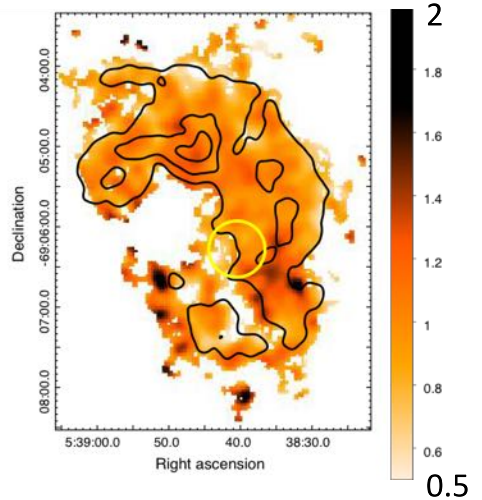

NGC 1569

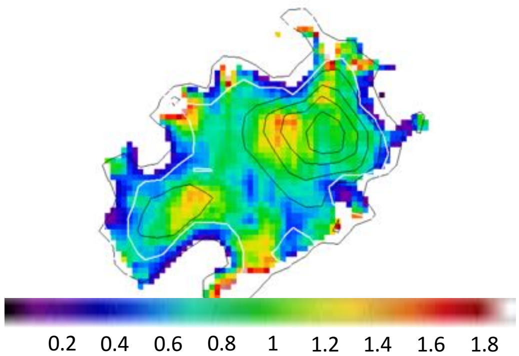

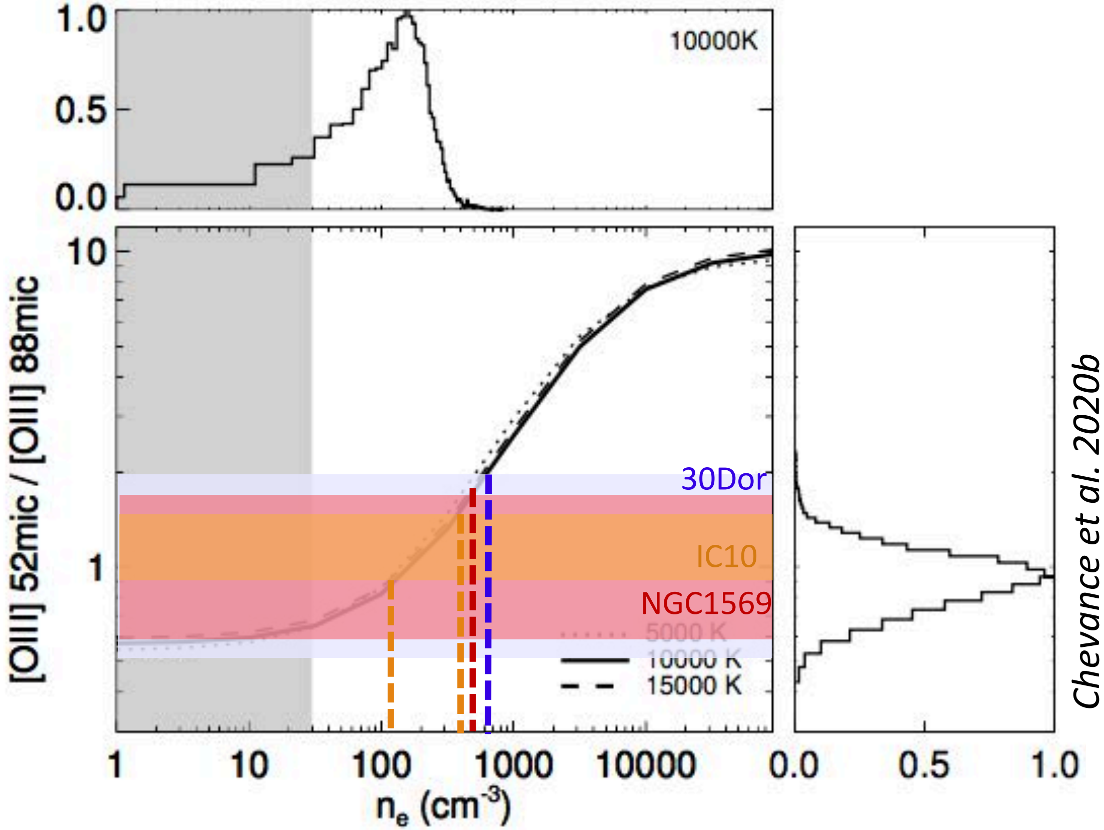

- ➢ 30Dor: electron density in the ionised gas < 600 cm^{-3}
- ➢ IC10: density ranges between 100 and 400 cm^{-3}
- ➢ NGC1569: electron density < 500 cm^{-3}

Empirical diagnostics:
Hardness of the radiation field

Dwarf Galaxy Survey

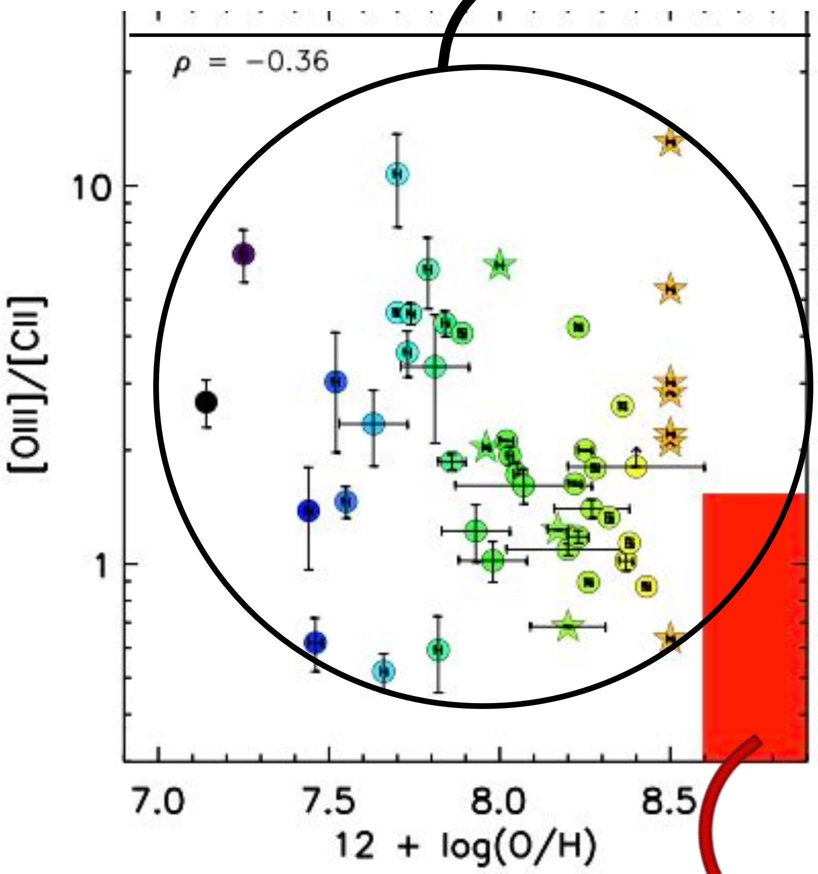

Cormier et al. 2015

Solar metallicity galaxies

Mélanie Chevance

Empirical diagnostics:
Hardness of the radiation field

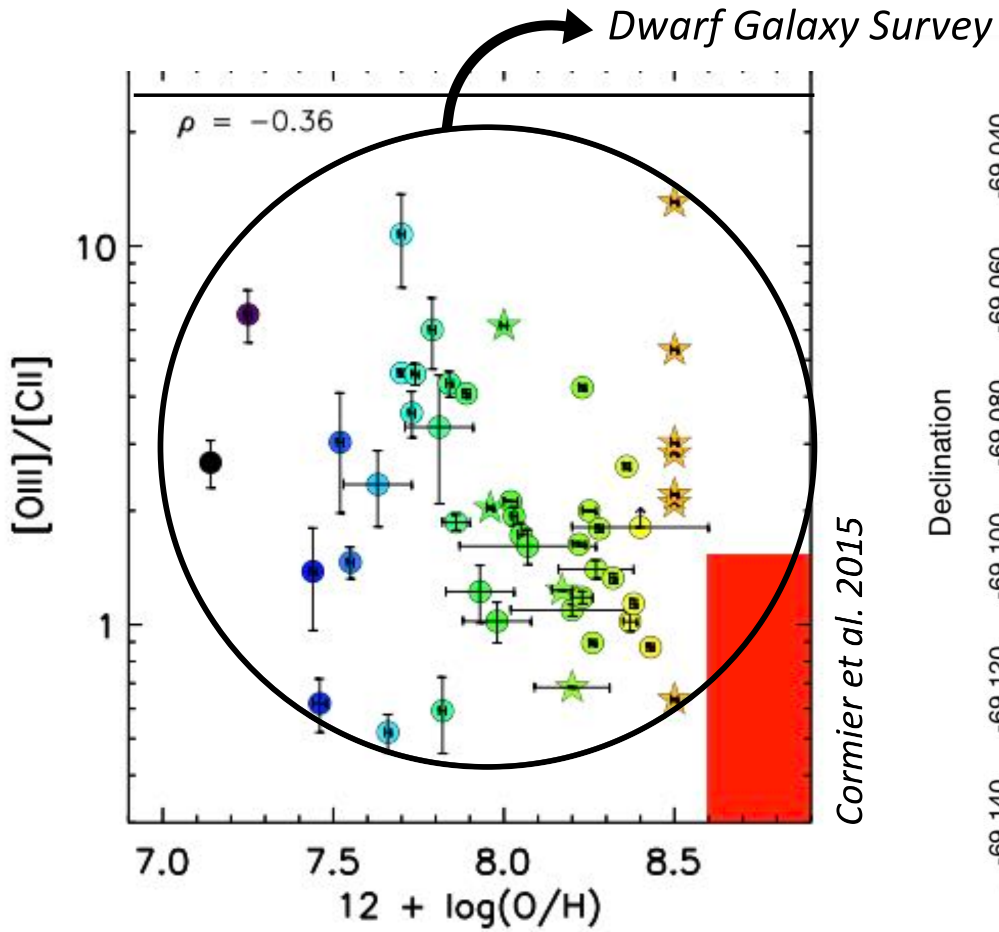

Cormier et al. 2015

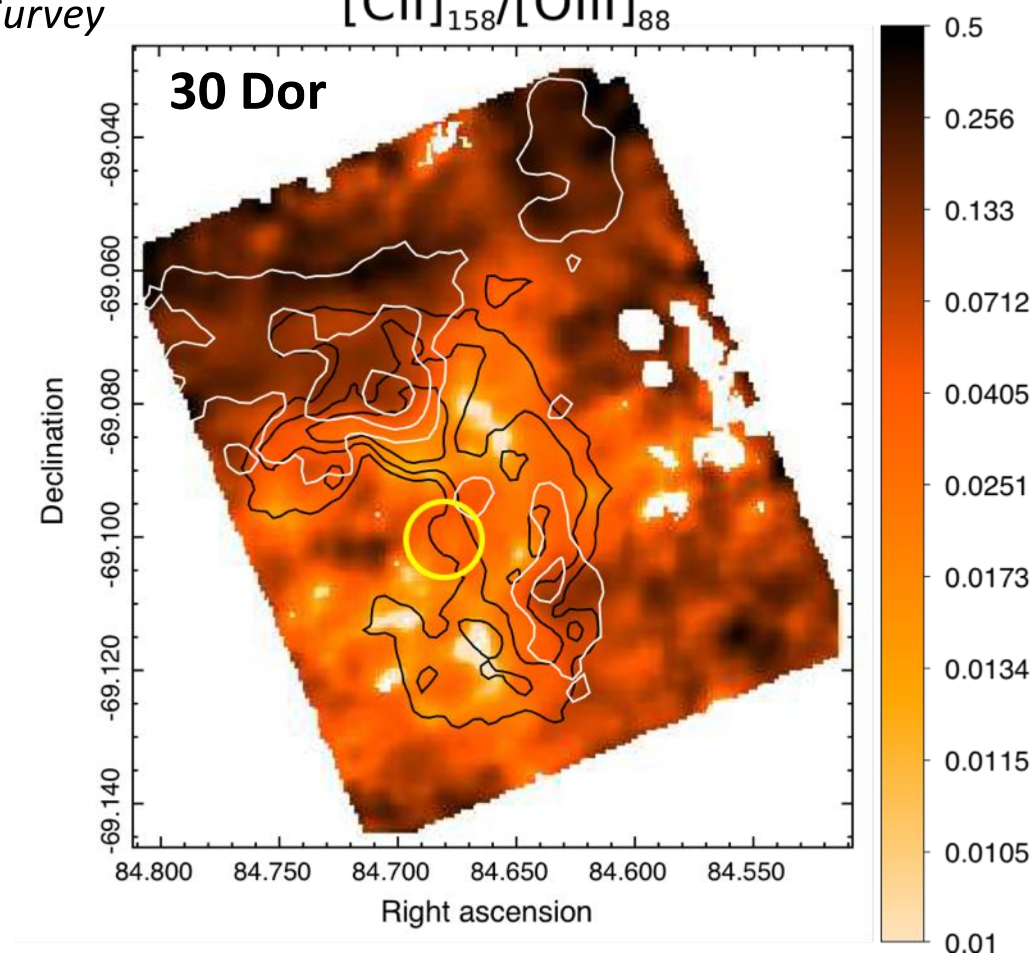

Chevance et al. 2020b

Empirical diagnostics:
Hardness of the radiation field

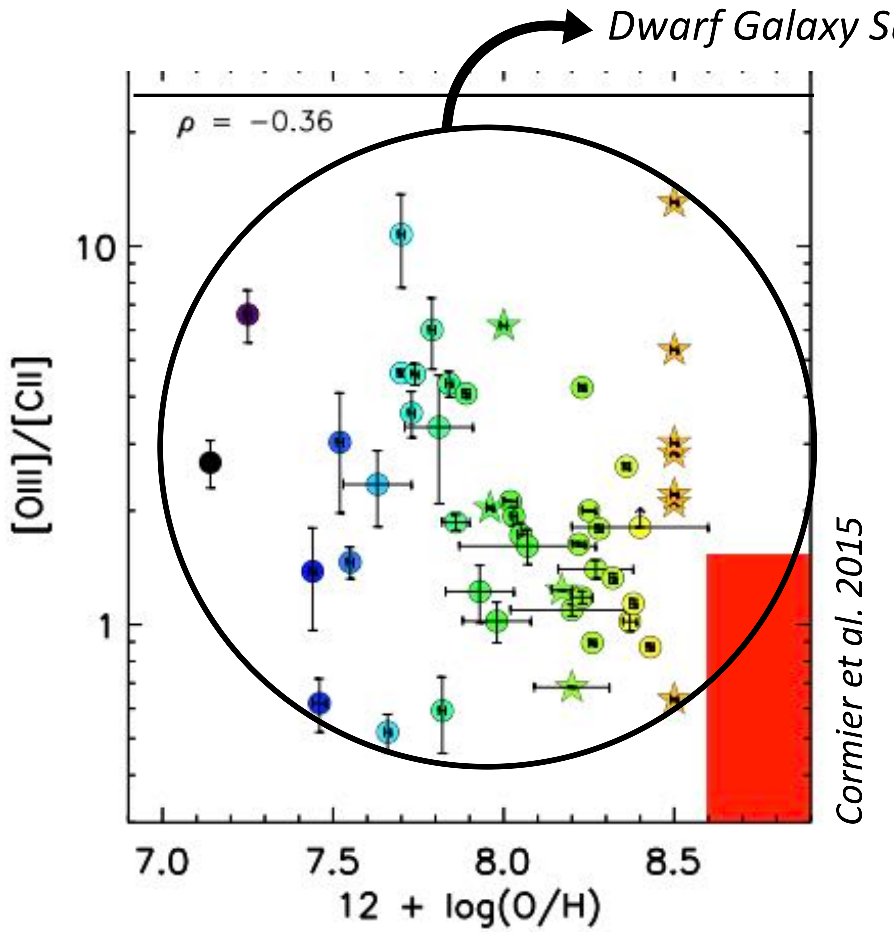

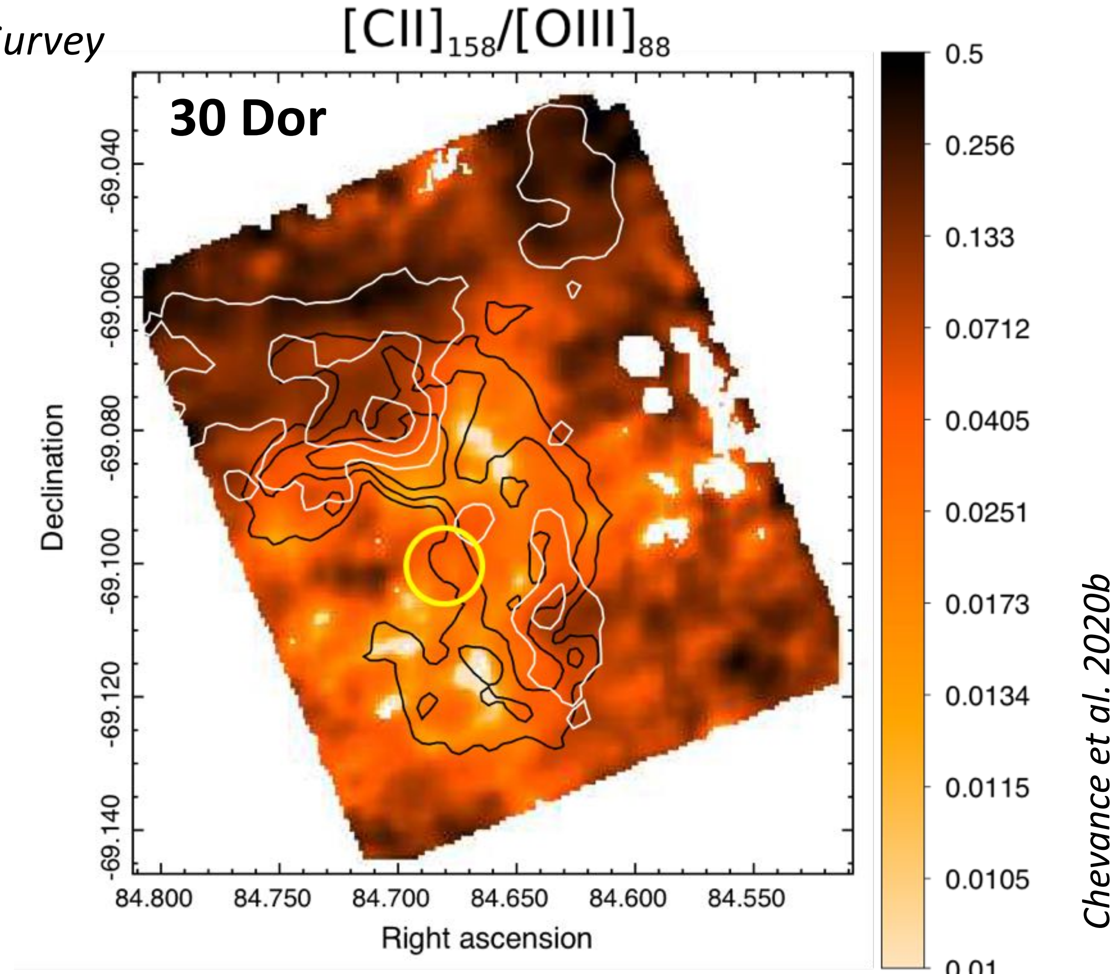

- ➢ The ISM becomes more porous towards lower metallicities

Empirical diagnostics:
Hardness of the radiation field

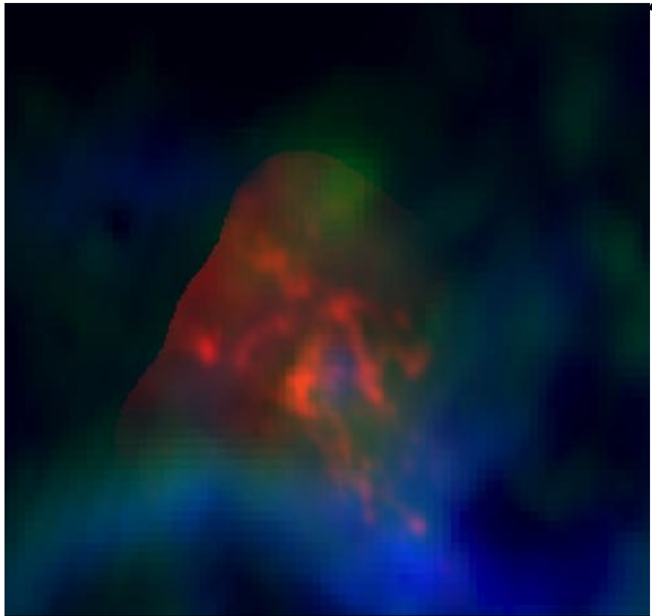

^{12}CO 2-1 (ALMA) R. Indebetouw
[NeIII], [SIV]: Spitzer IRS (Indebetouw + 09)

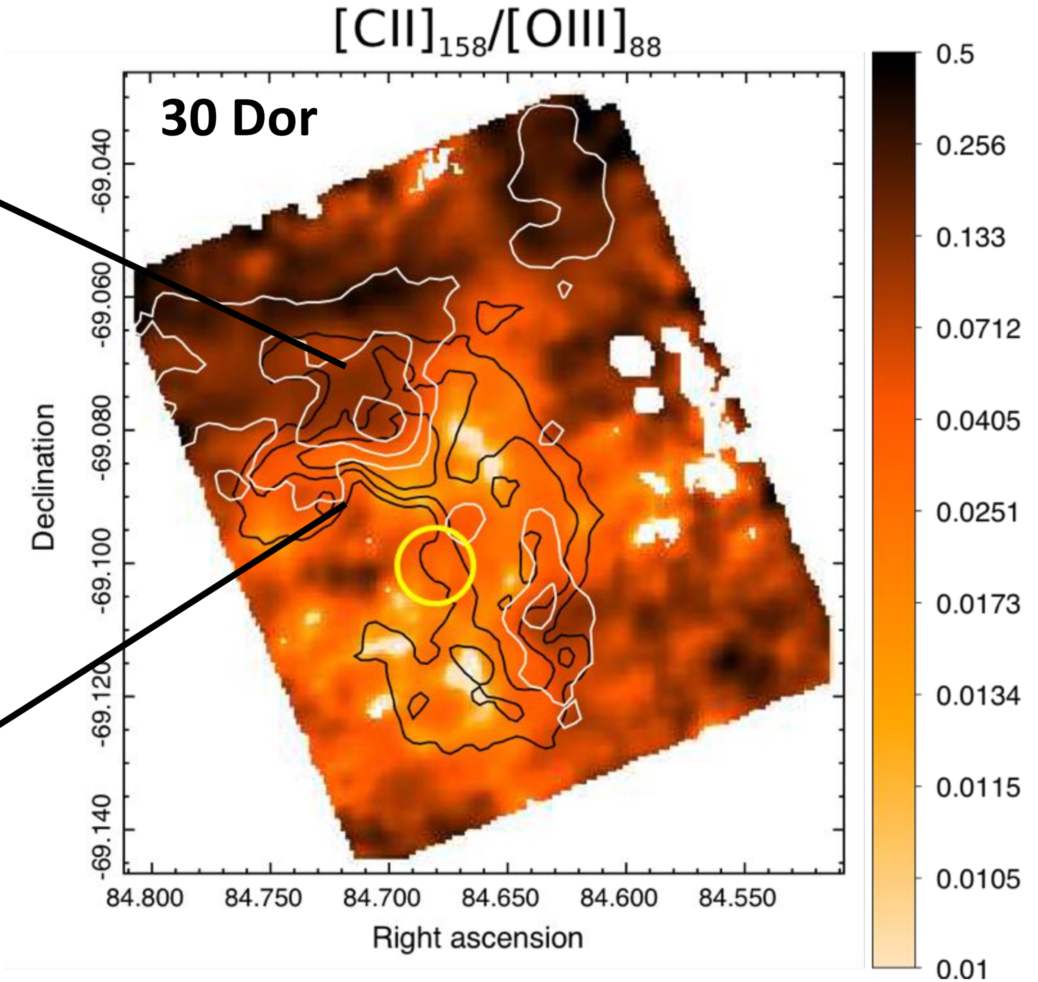

Chevance et al. 2020b

Modelling of the structure and physical conditions of the gas

The Meudon PDR code *(Le Petit et al. 2006, Le Bourlot et al. 2014, Bron et al. 2014)*

<u>Model characteristics</u>:
- Parallel slab geometry
- Gas phase abundances measured in 30Dor *(Pellegrini+2011)*
- Constant pressure

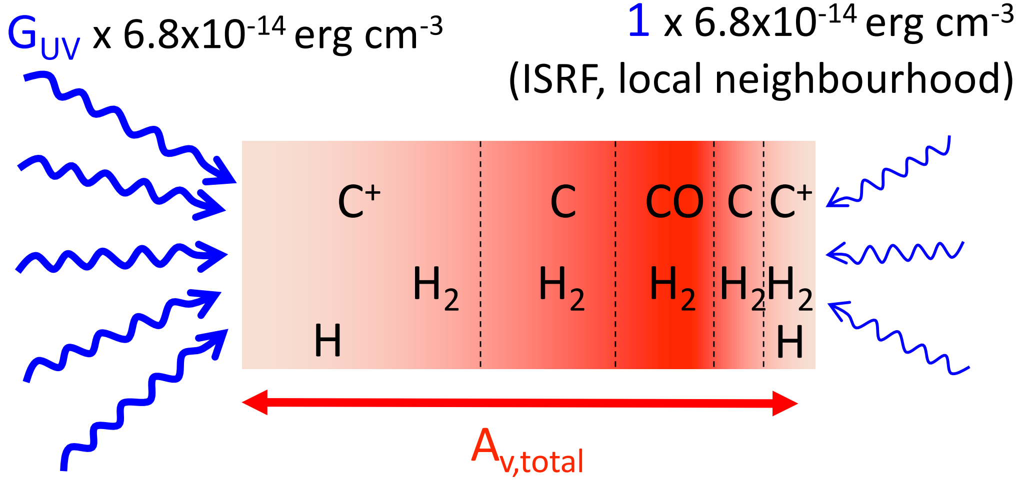

Modelling of the structure and physical conditions of the gas

The Meudon PDR code *(Le Petit et al. 2006, Le Bourlot et al. 2014, Bron et al. 2014)*

Model characteristics:
- Parallel slab geometry
- Gas phase abundances measured in 30Dor *(Pellegrini+2011)*
- Constant pressure

Key parameters:
- G_{UV}: intensity of the *incident* radiation field
- P: pressure of the cloud
- $A_{v,total}$: visual extinction

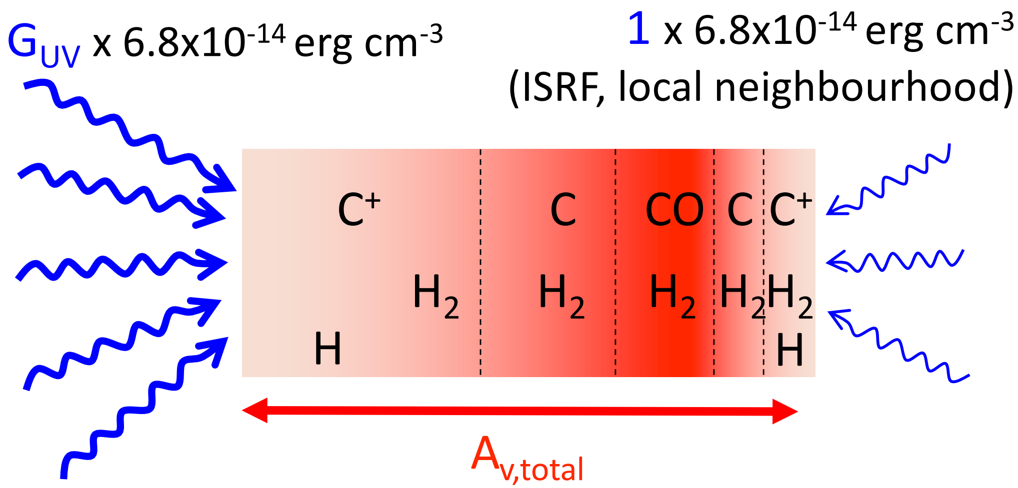

Modelling of the structure and physical conditions of the gas

The Meudon PDR code *(Le Petit et al. 2006, Le Bourlot et al. 2014, Bron et al. 2014)*

Model characteristics:

- Parallel slab geometry
- Gas phase abundances measured in 30Dor *(Pellegrini+2011)*
- Constant pressure

Key parameters:

- G_{UV}: intensity of the *incident* radiation field
- P: pressure of the cloud
- $A_{v,total}$: visual extinction

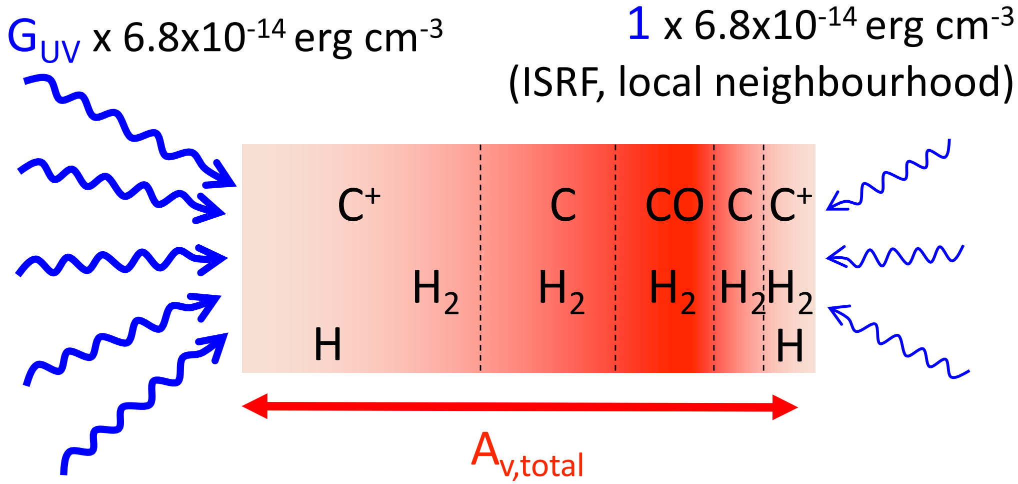

G_{UV}, P: Constrained by [CII], [OI], L_{FIR}

$A_{v,total}$: Constrained by the ratios [CI]/[CII] or CO/[CII]

Modelling of the structure and physical conditions of the gas

30 Dor

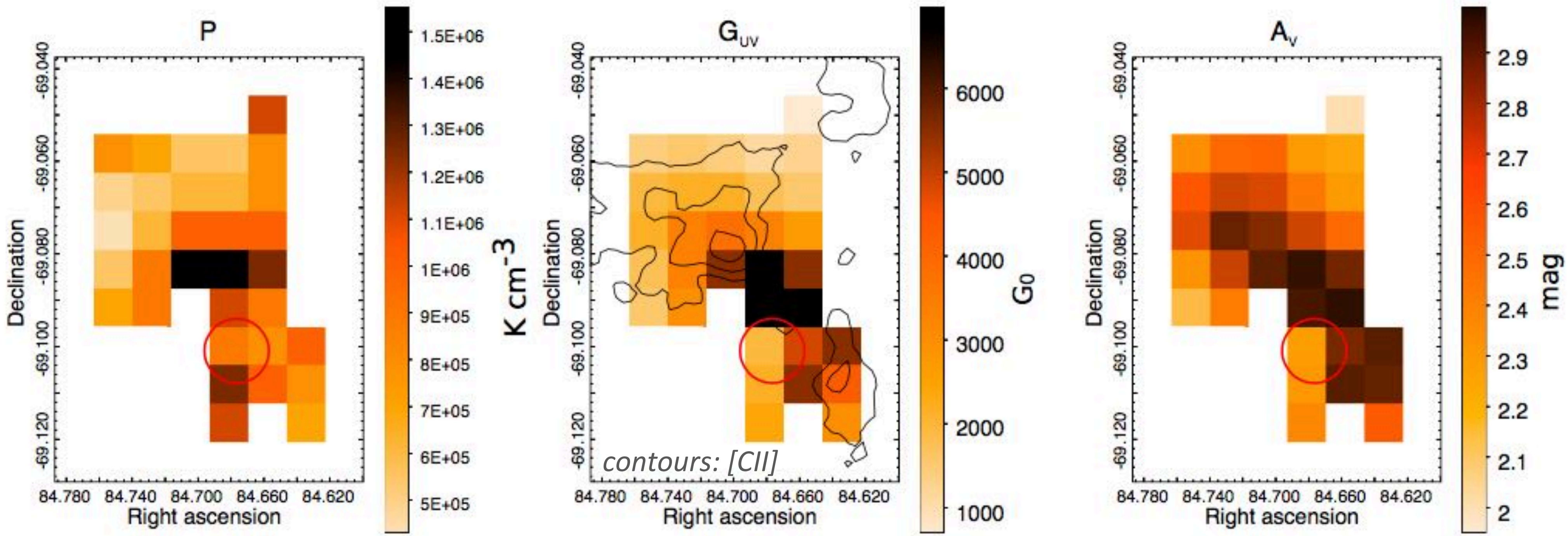

Chevance et al. 2016
Chevance et al. 2020b

Physical distance between stars and clouds : a 3D view of 30Dor

G_{UV}

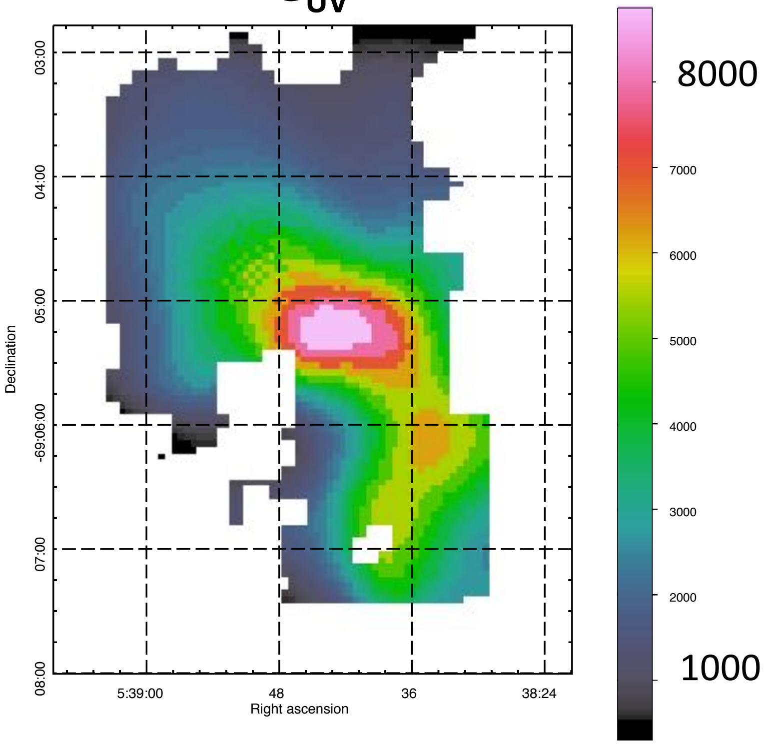

Emitted G_{stars} from the cluster

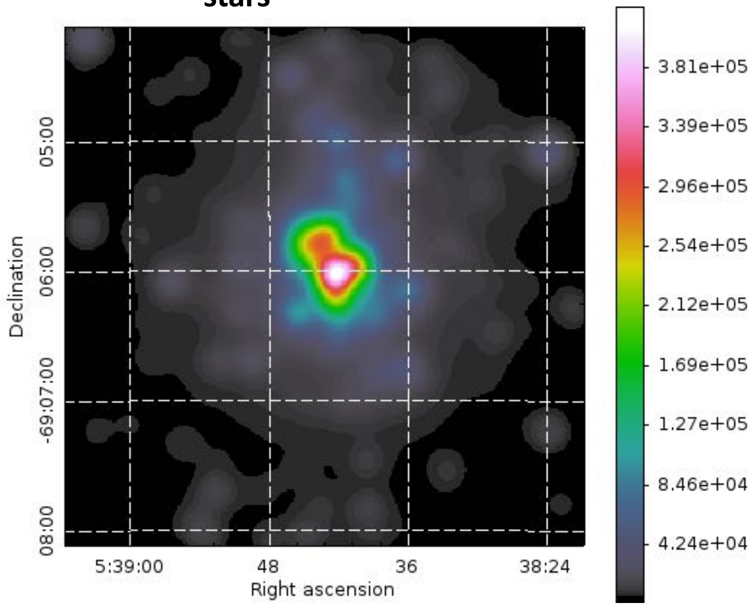

Physical distance to the center of the cluster

$$G_{stars} = G_{UV} \times \frac{L^2}{d^2}$$

Projected distance

Physical distance between stars and clouds: a 3D view of 30Dor

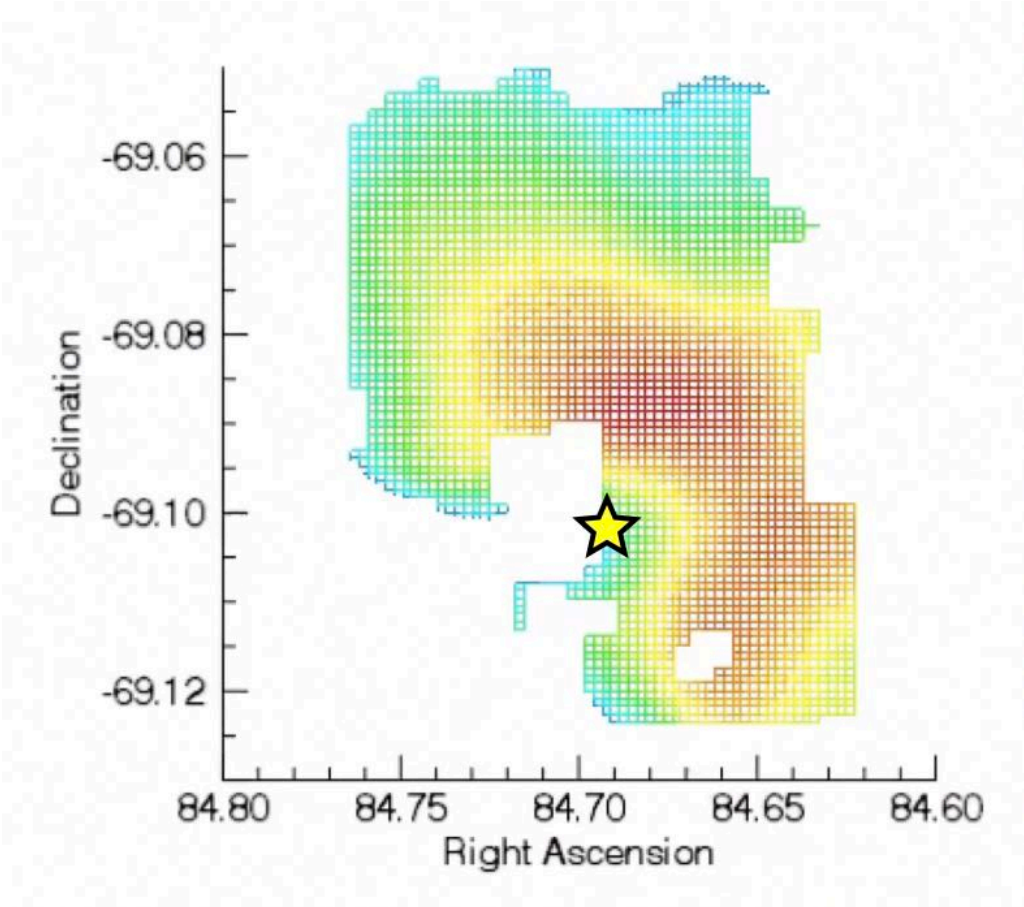

Chevance et al. 2016
Chevance et al. 2020b

Physical distance between stars and clouds: a 3D view of 30Dor

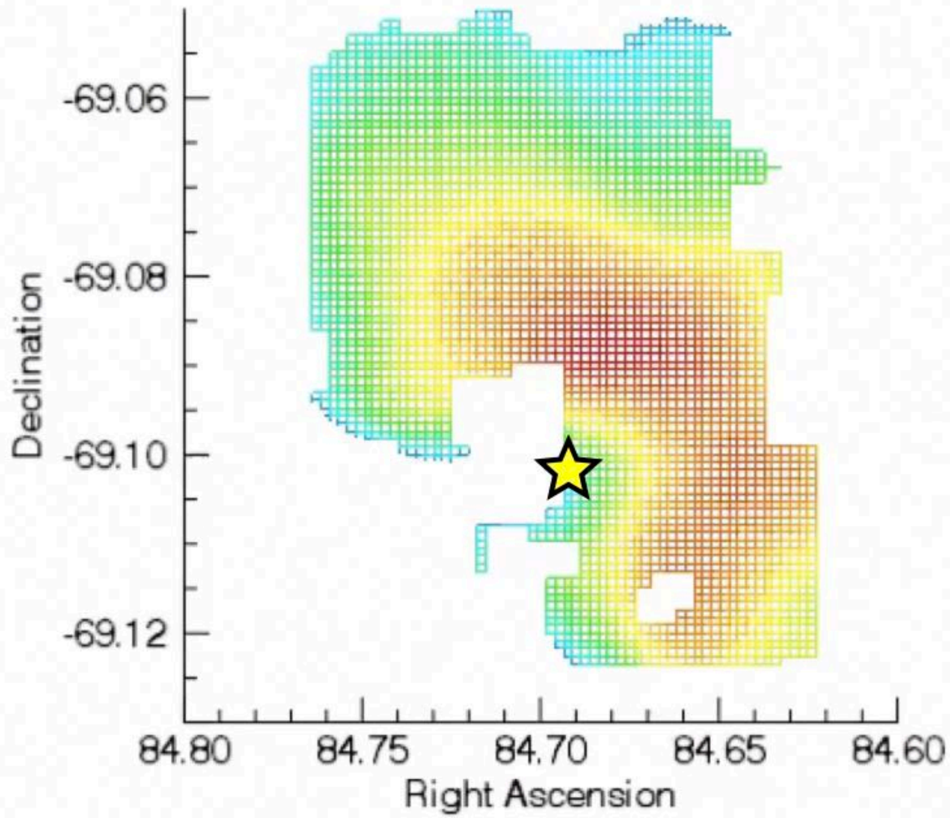

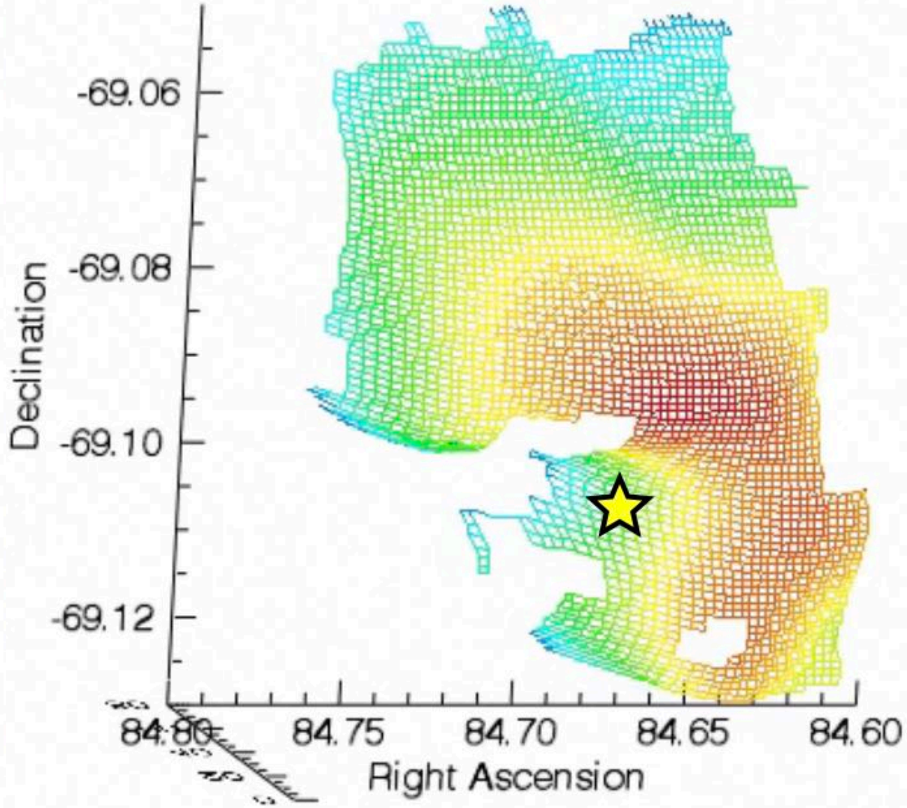

Chevance et al. 2016
Chevance et al. 2020b

What is the total reservoir of molecular gas?

Total H_2 mass
predicted by the PDR model

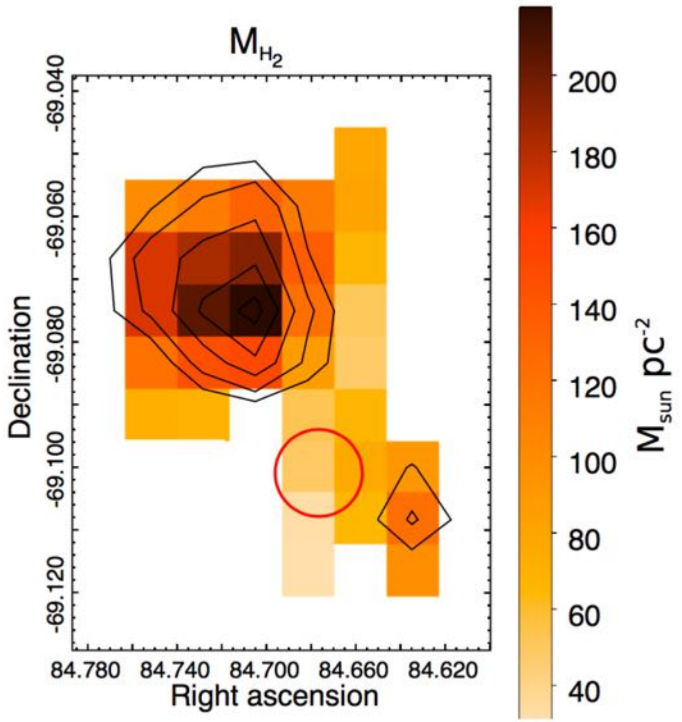

Chevance et al. 2020b

What is the total reservoir of molecular gas?

Total H_2 mass
predicted by the PDR model

$$N(H_2) = X_{CO} \times I_{CO}$$

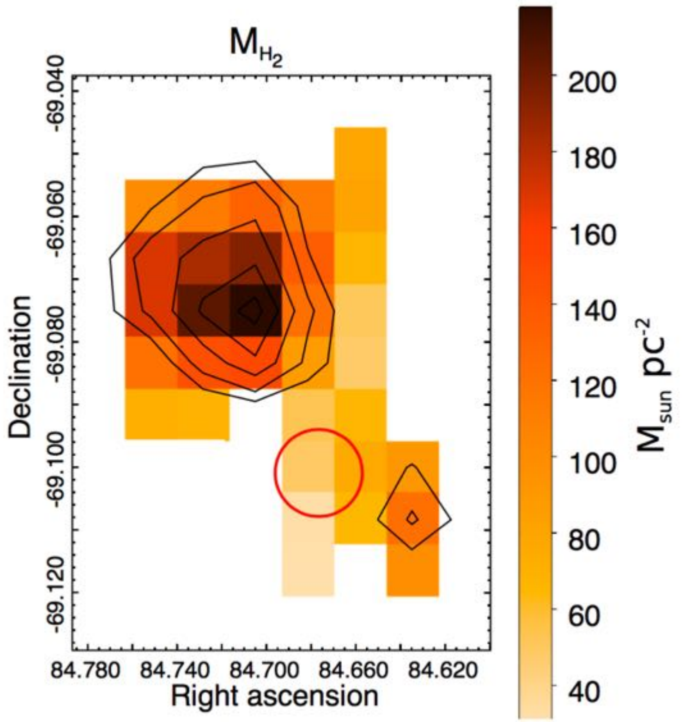

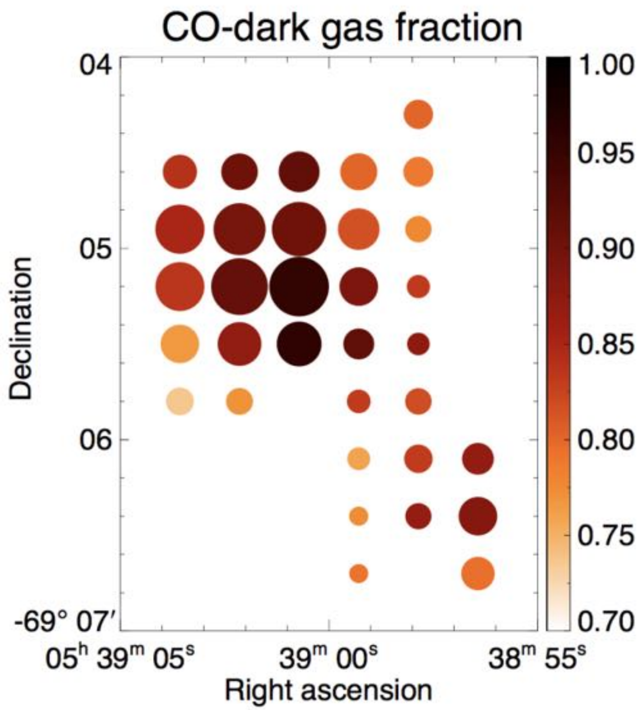

Chevance et al. 2020b

What is the total reservoir of molecular gas?

Total H_2 mass
predicted by the PDR model

$$N(H_2) = X_{CO} \times I_{CO}$$

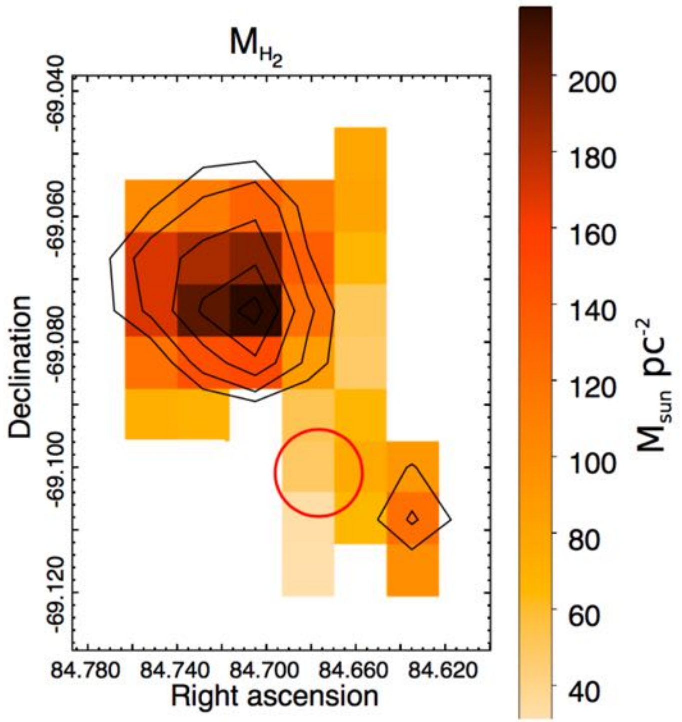

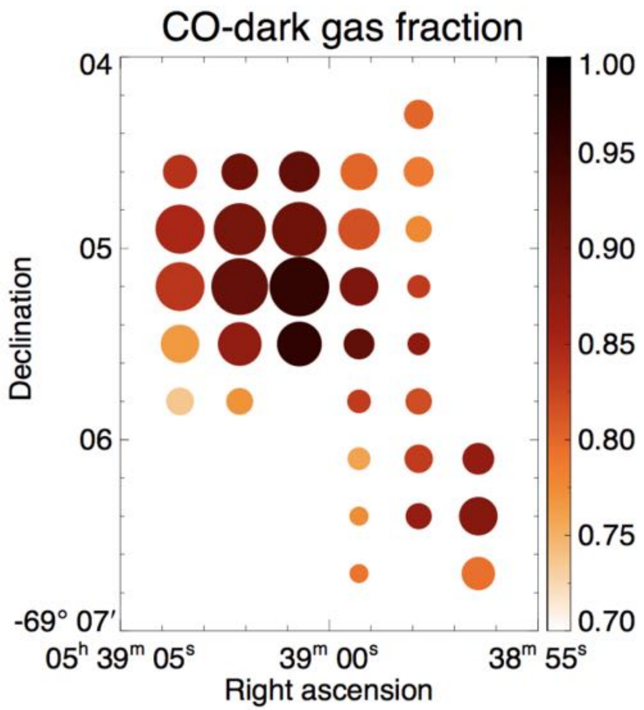

- More than 75% of the molecular gas **not traced by CO**

Chevance et al. 2020b

What is the total reservoir of molecular gas?

Total H_2 mass predicted by the PDR model

$$N(H_2) = X_{CO} \times I_{CO}$$

$$X_{CO}(30Dor) = \frac{N(H_2)}{I_{CO}}$$

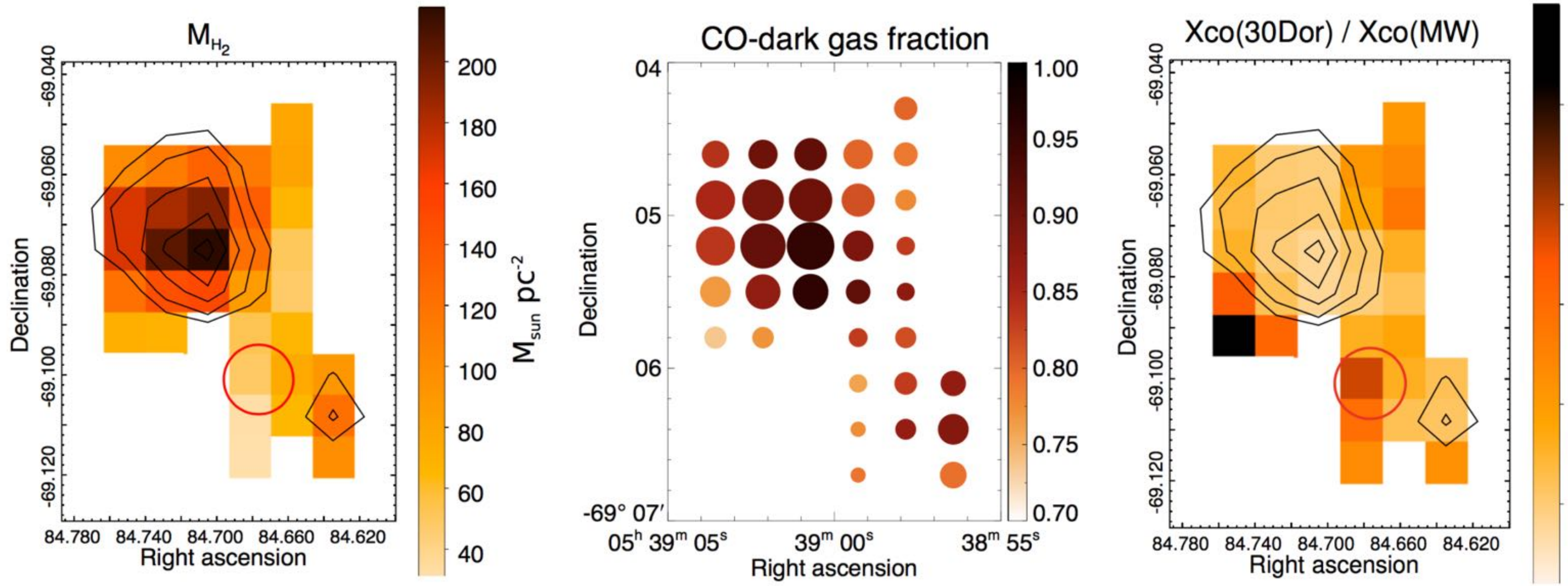

Chevance et al. 2020b

Environmental variations of the CO-dark gas mass

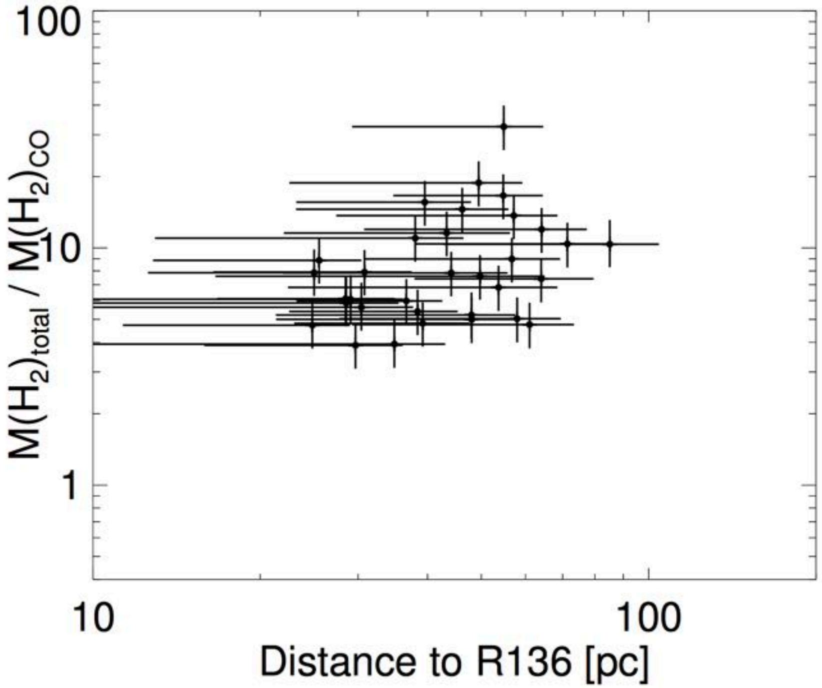

➢ The **fraction of CO-dark gas is smaller closer** to R136 (at high radiation field)

Mélanie Chevance

Environmental variations of the CO-dark gas mass

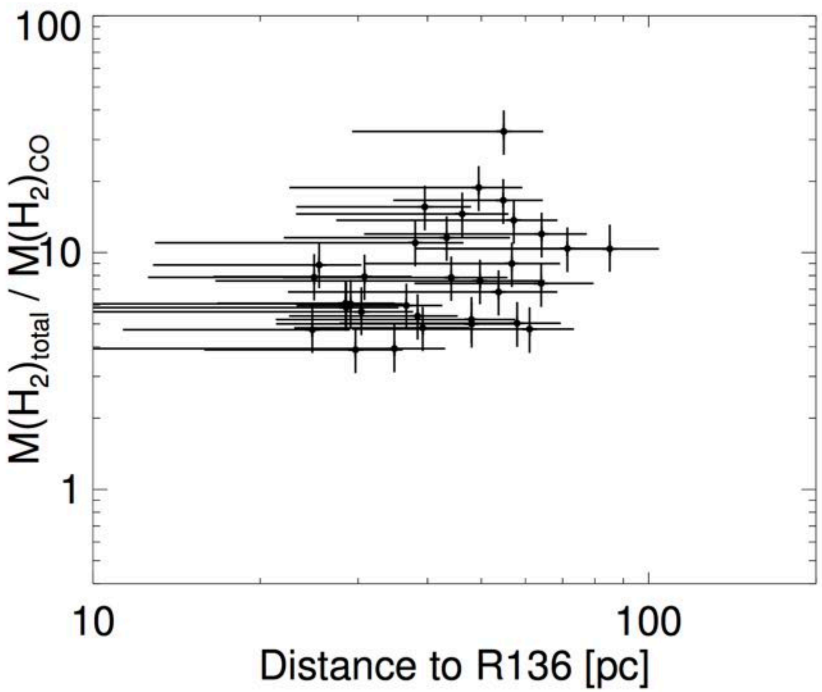

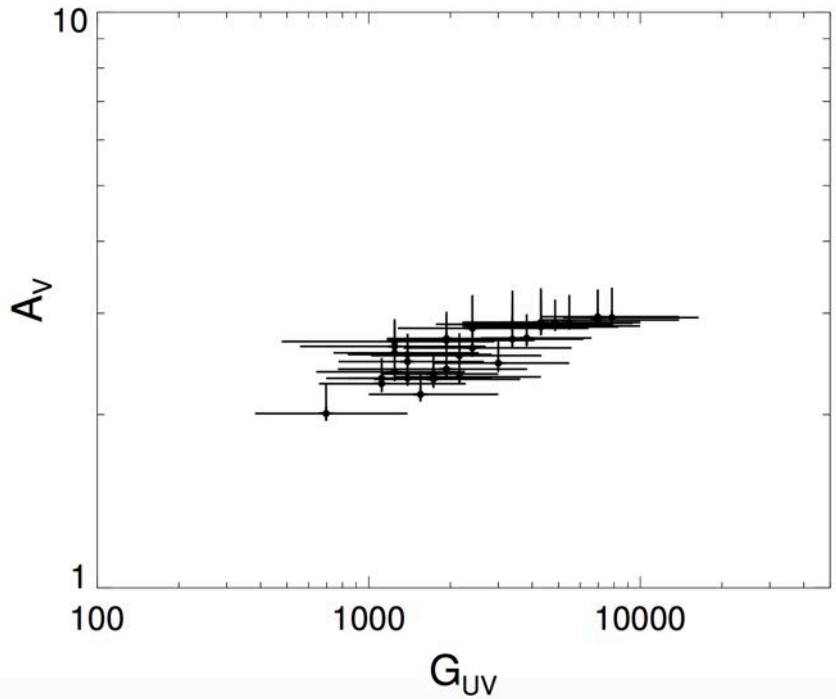

- The **fraction of CO-dark gas is smaller closer** to R136 (at high radiation field)
- Due to the fact that **clouds close to R136** (high radiation field) **have higher A_V**

Environmental variations of the CO-dark gas mass

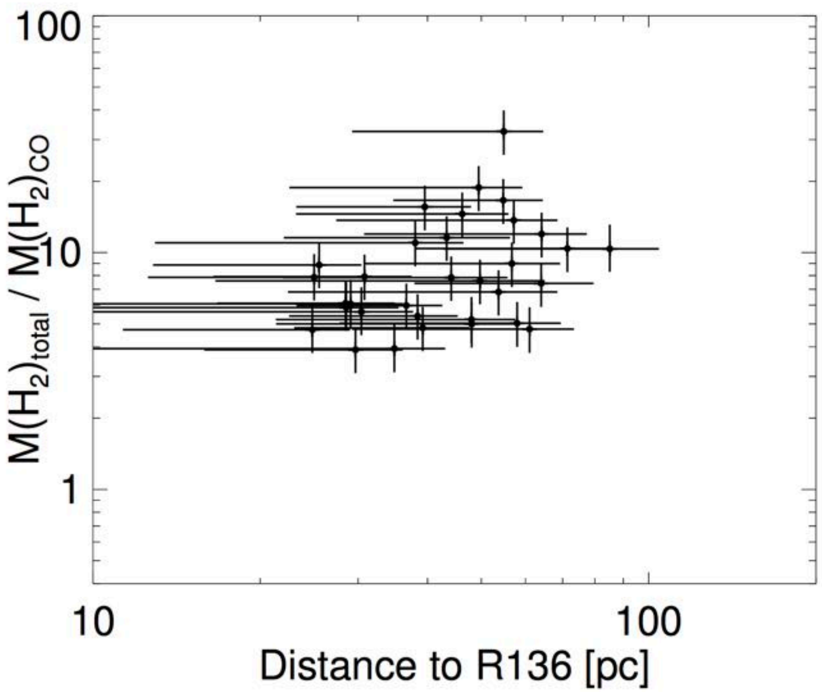

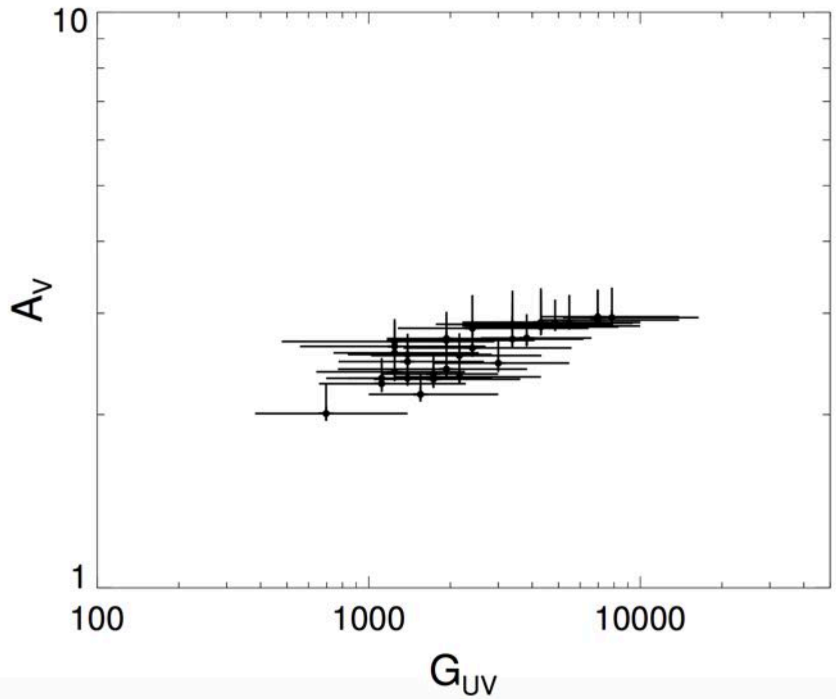

- The **fraction of CO-dark gas is smaller closer** to R136 (at high radiation field)
- Due to the fact that **clouds close to R136** (high radiation field) **have higher A_V**
- At higher A_V, the CO-free molecular envelope represents a smaller fraction of the total cloud mass

Tracing the total molecular gas with [CII]

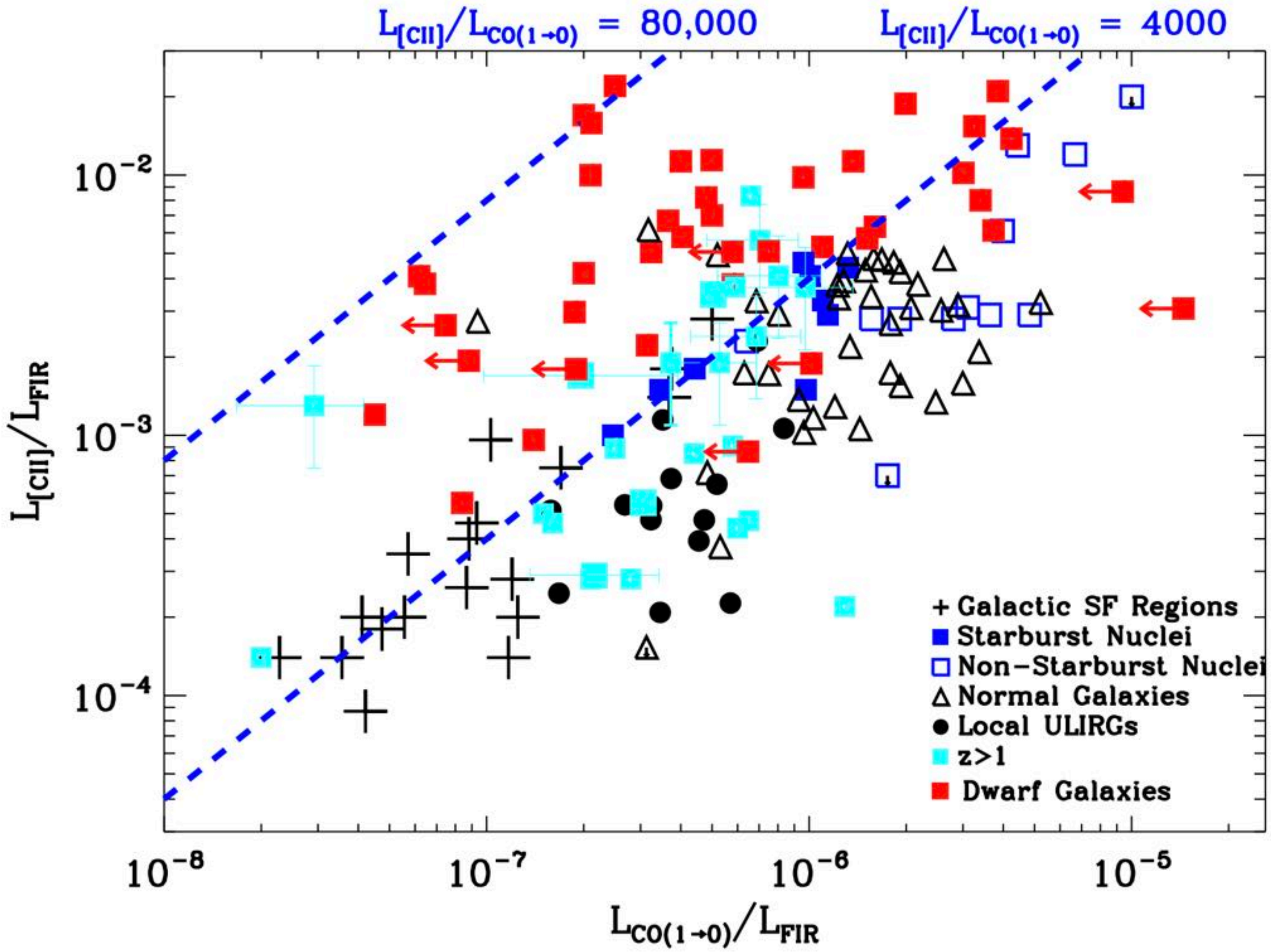

Madden et al. (2020)

Tracing the total molecular gas with [CII]

Model predictions show that:

- **[CI] and [CII]** are good tracer of the molecular gas at low metallicity
- **[CII] is a better tracer** due to its higher luminosity

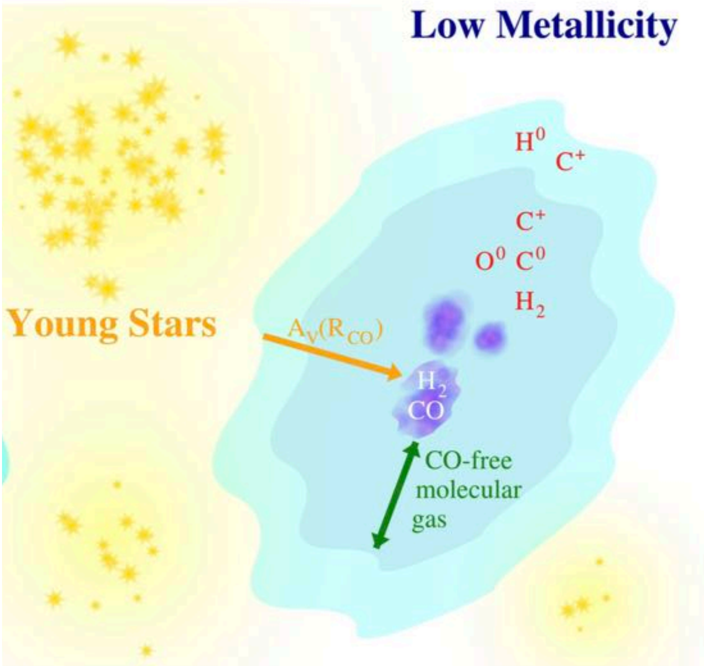

Madden et al. (2020)

Tracing the total molecular gas with [CII]

Model predictions show that:

- **[CI] and [CII]** are good tracer of the molecular gas at low metallicity
- **[CII] is a better tracer** due to its higher luminosity

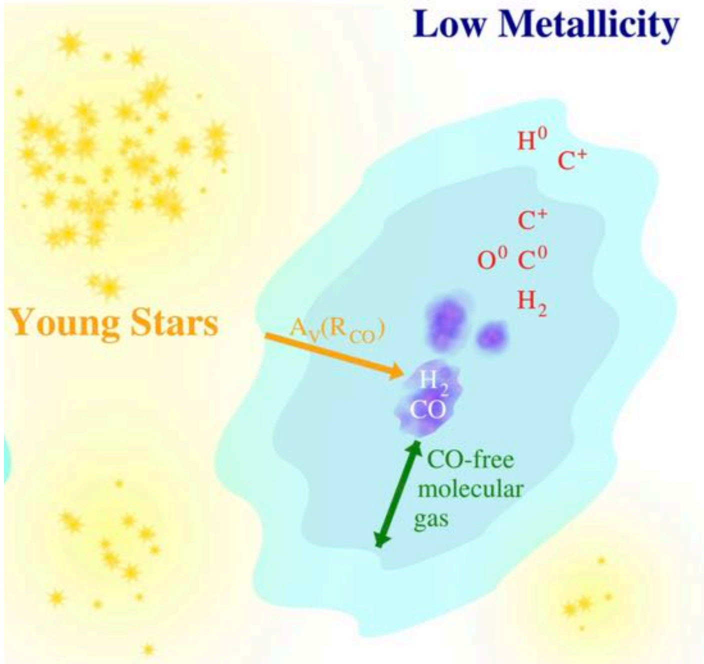

Madden et al. (2020)

Madden et al. (2020) used a photoionisation model to **determine systematically the CO-dark molecular gas mass from [CII]** observations:

- $M(H_2)_{total} = 10^{2.12} \times [L_{[C\ II]}]^{0.97}$
- $\alpha_{CO} = 10^{0.58} \times [Z/Z_{\odot}]^{-3.39}$

Tracing the total molecular gas with [CII]

Star formation relation

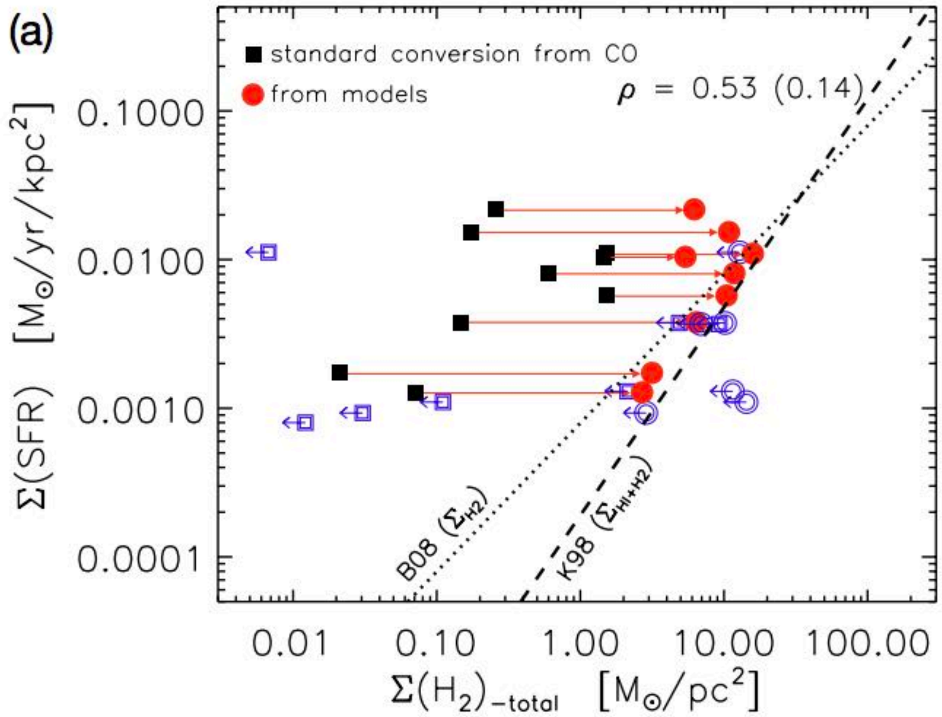

Madden et al. (2020)

- Low-metallicity galaxies back on the standard star-formation relation

Tracing the total molecular gas with [CII]

Star formation relation

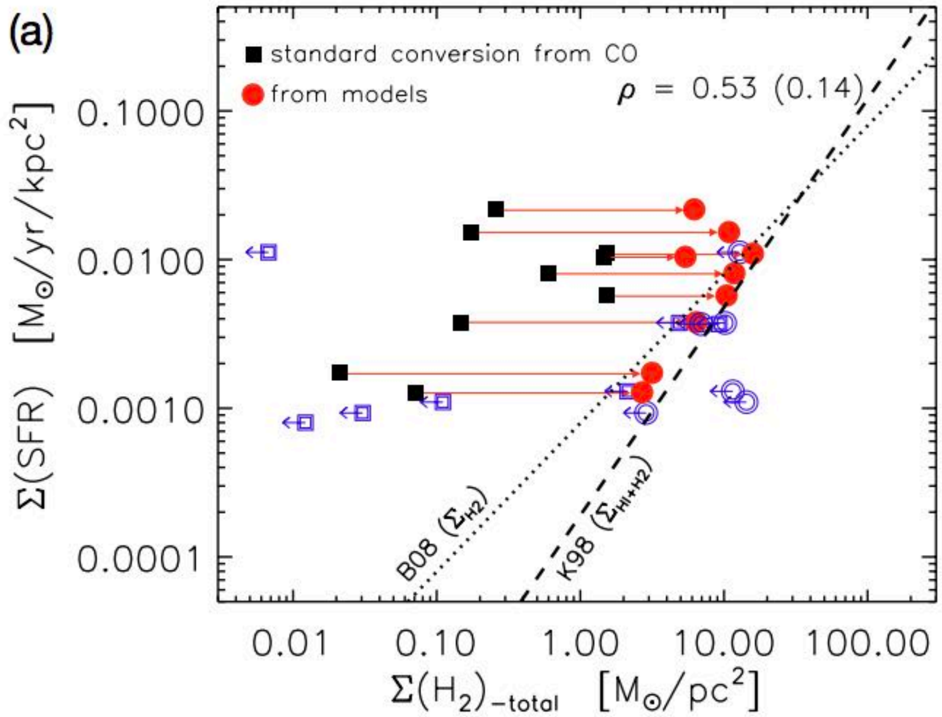

CO-to-H_2 conversion factor

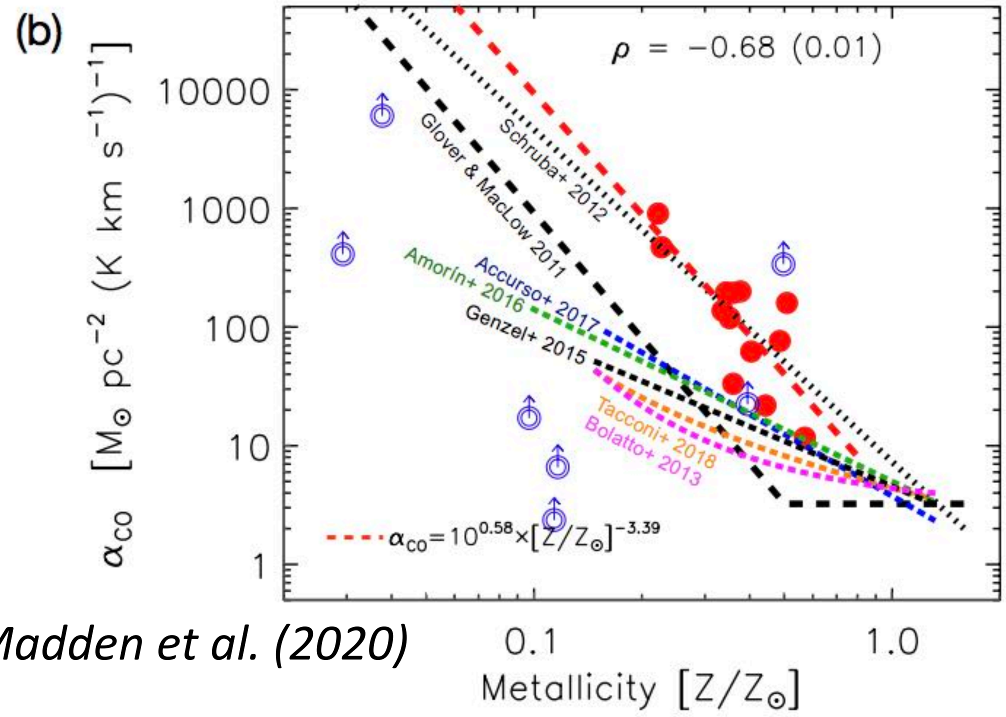

Madden et al. (2020)

- Low-metallicity galaxies back on the standard star-formation relation
- Steep slope of the CO-to-H_2 conversion factor with metallicity

How can we understand this slope?

- Based on the elemental abundances only, we expect CO abundance to scale ~ linearly with metallicity

How can we understand this slope?

- Based on the elemental abundances only, we expect CO abundance to scale ~ linearly with metallicity

- The observed slope of α_{CO} with Z is -3.39, much steeper than -1

- How can we explain this?

How can we understand this slope?

- This can potentially be explained by an environmental dependent radiation field dissociating CO (H_2 self-shielded)

How can we understand this slope?

- This can potentially be explained by an environmental dependent radiation field dissociating CO (H_2 self-shielded)

- Can the UV photons emitted by young star-forming regions be responsible?

How can we understand this slope?

- This can potentially be explained by an environmental dependent radiation field dissociating CO (H_2 self-shielded)

- Can the UV photons emitted by young star-forming regions be responsible?

- How many photons escape during a star-forming region lifetime?

Evolutionary cycle between clouds, feedback phase and young stellar regions

➢ We have linked the spatial decorrelation between **CO and Hα** to their **emission timescale**

Kruijssen et al. (2018), Hygate et al. (2019), Haydon et al. (2020b)

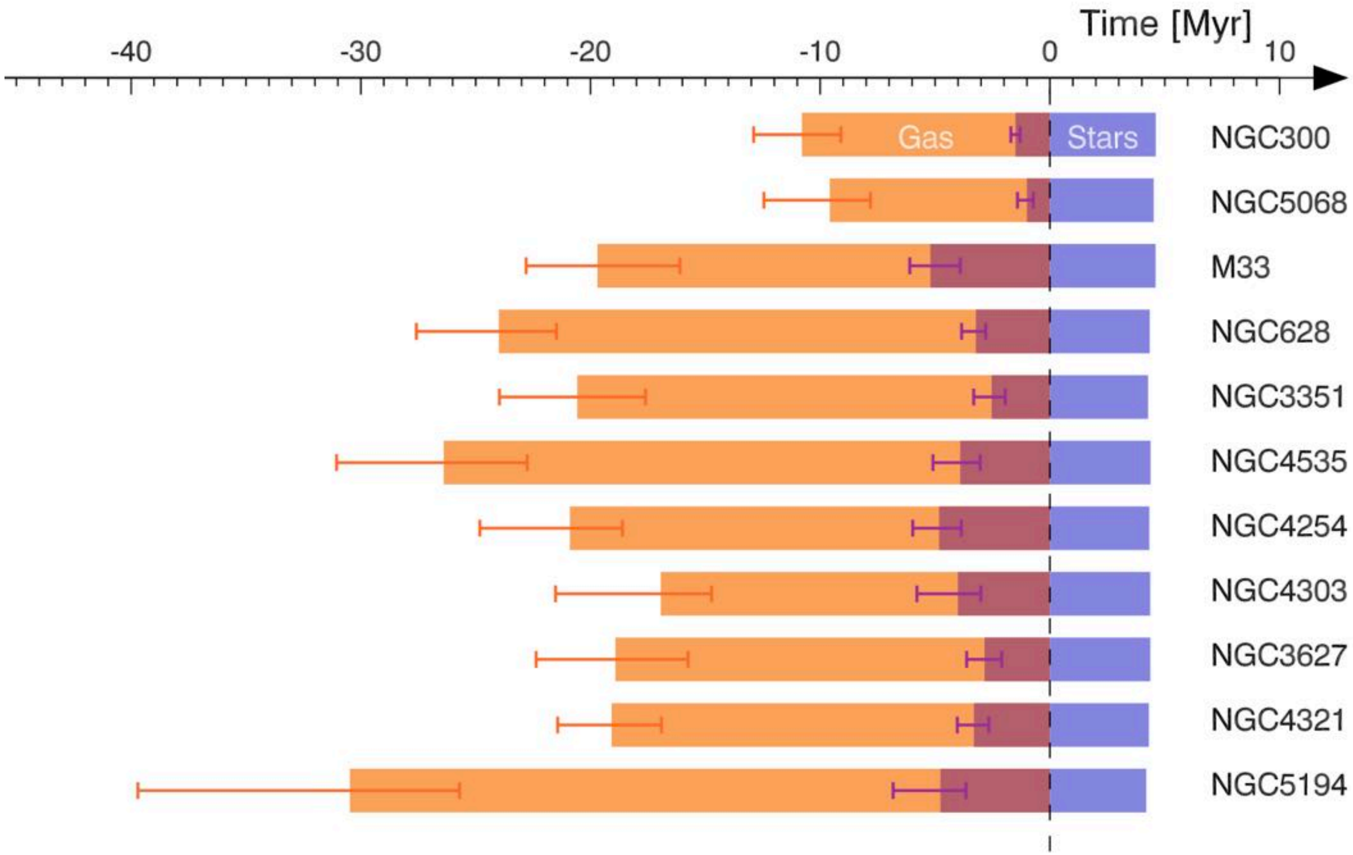

Chevance et al. (2020a,c)

The observed "feedback timescale" exceeds the predicted timescale

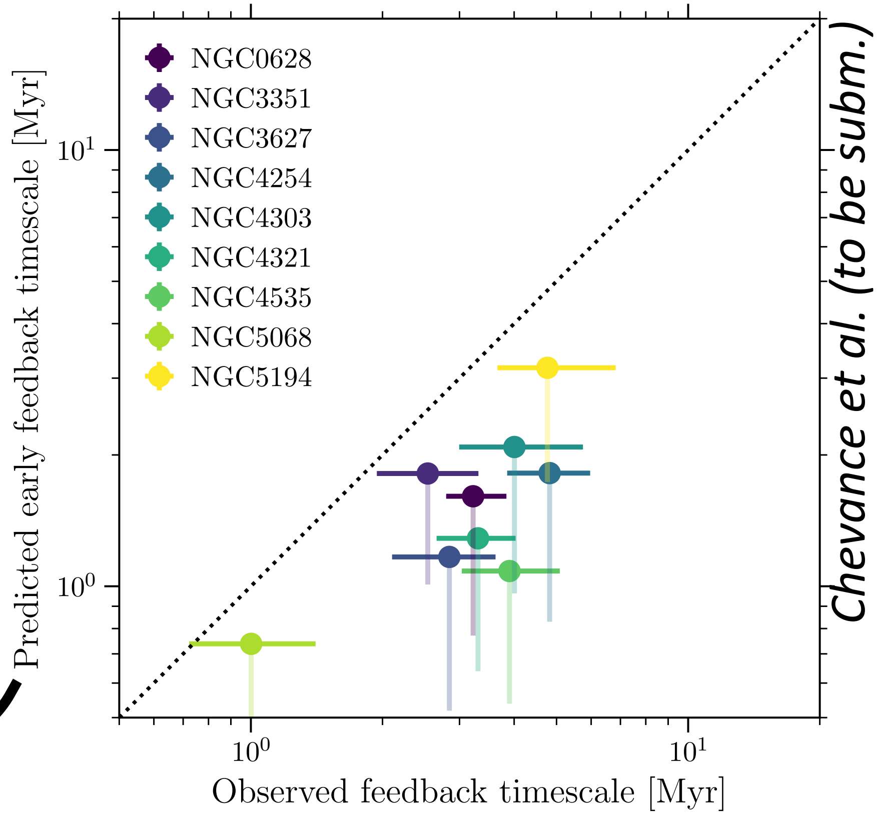

if all emitted photons couple to the parent cloud

The observed "feedback timescale" exceeds the predicted timescale

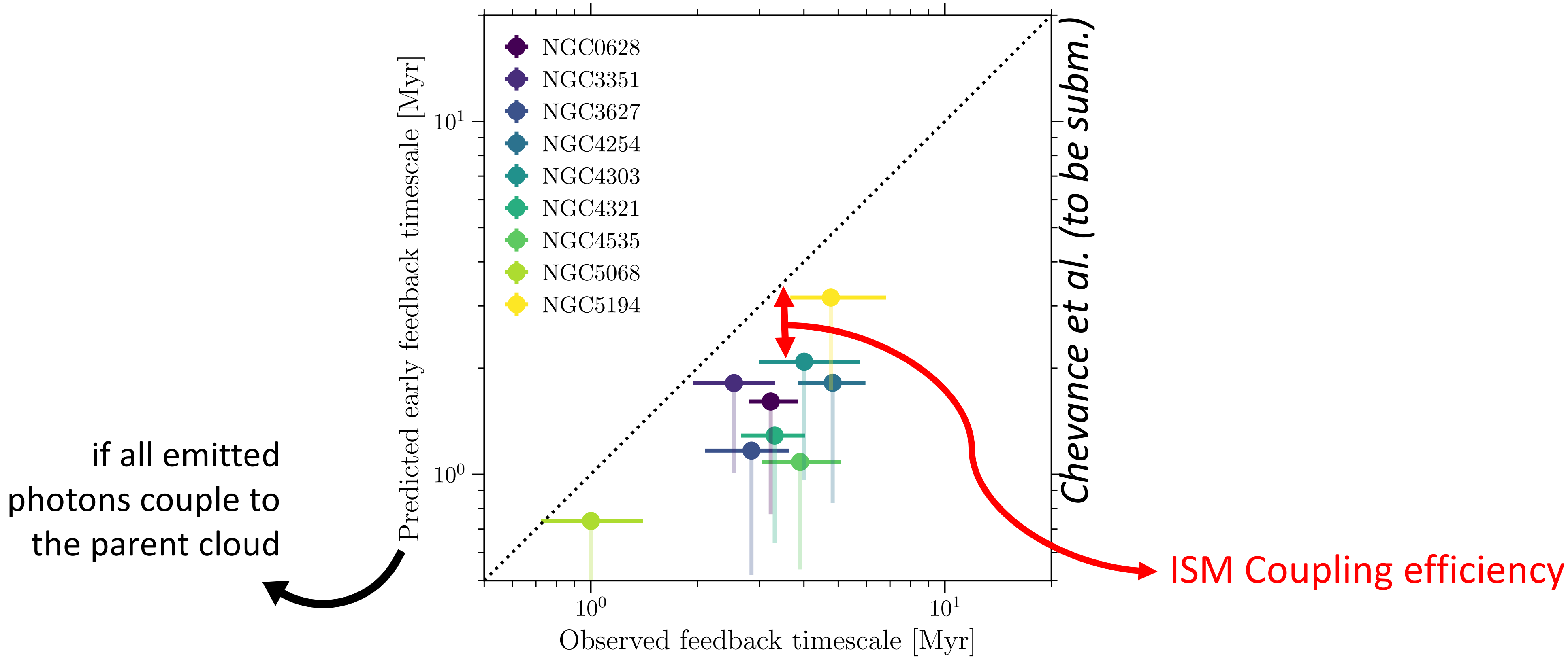

- Offset reflects the coupling efficiency between feedback and the surrounding ISM

Coupling efficiency as a function of metallicity

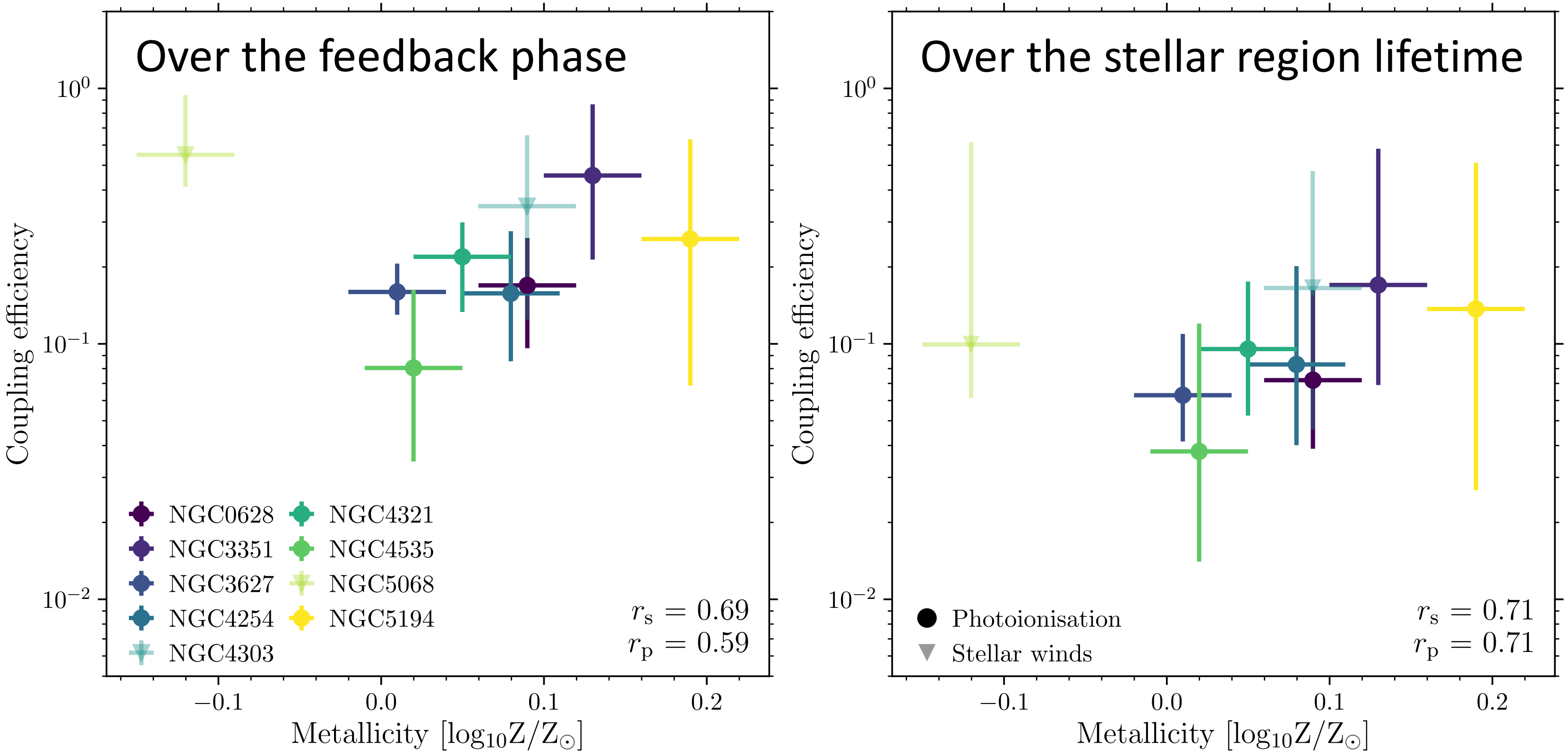

Chevance et al. (to be subm.)

Coupling efficiency as a function of metallicity

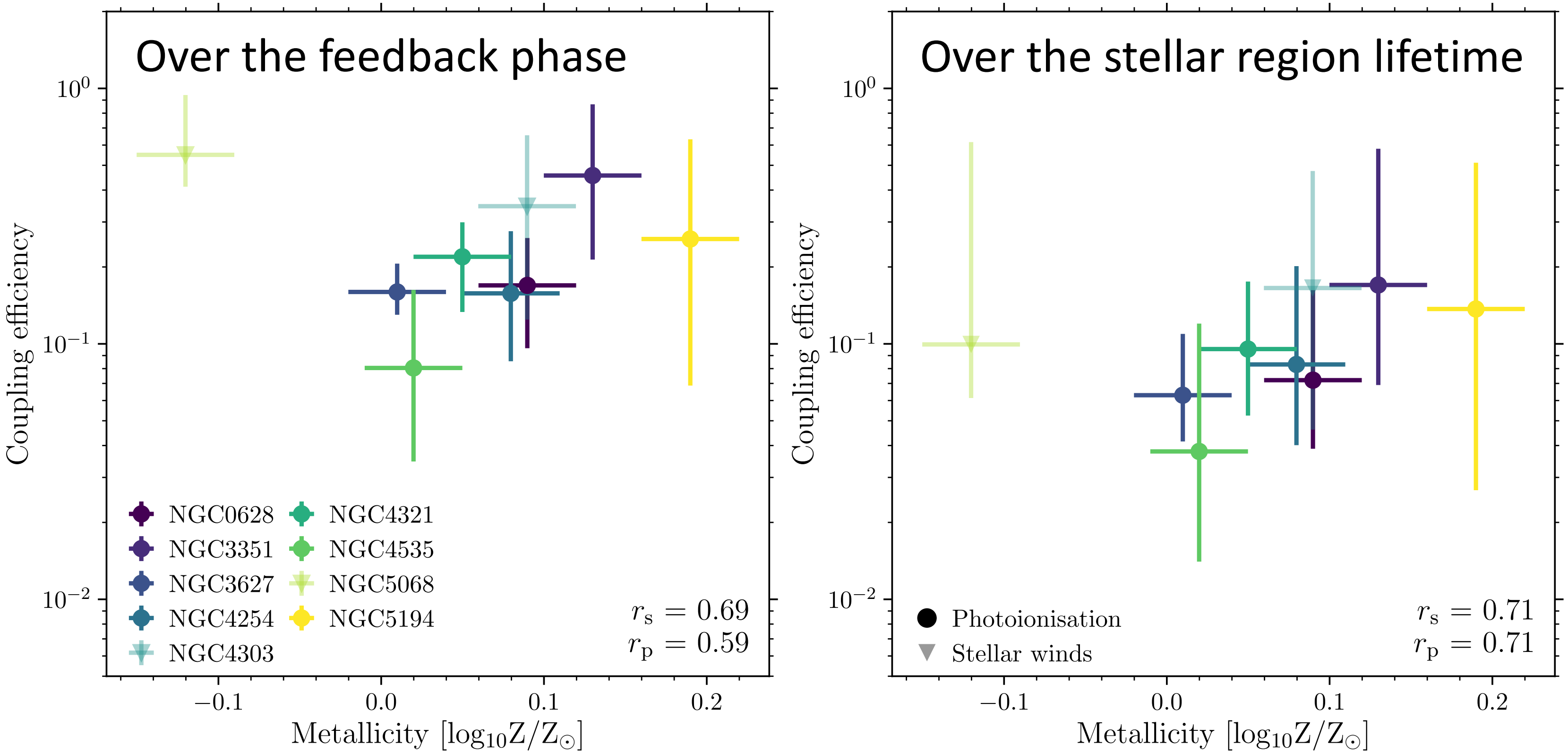

Chevance et al. (to be subm.)

- **Photoionisation** as a source of feedback **couples more efficiently** with the ISM at **high metallicity -> more photons escape at lower metallicity**

Metallicity dependence of the CO-to-H_2 conversion factor

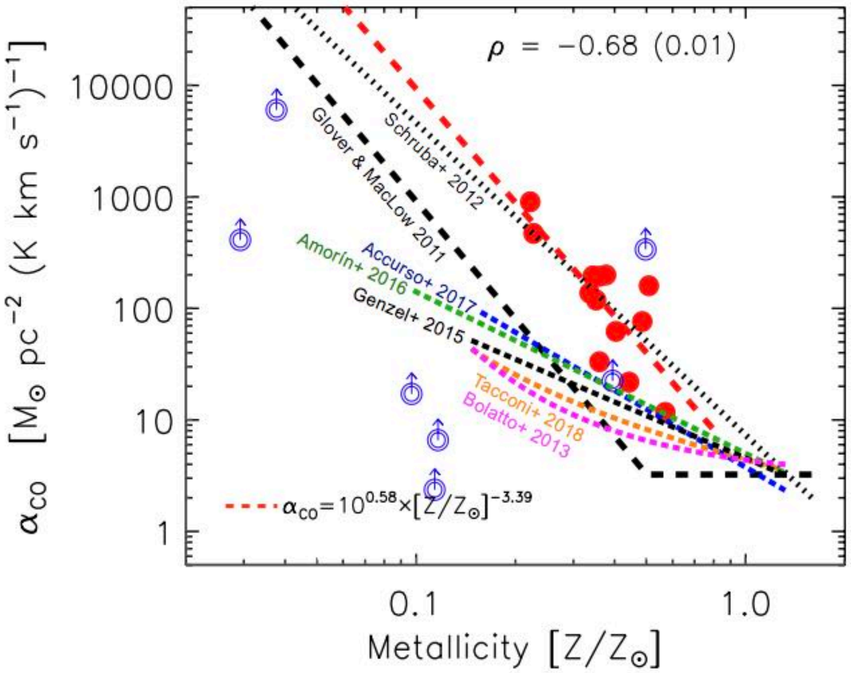

Madden et al. (2020)

- The low CO/SFR and high [C II]/CO observed in low metallicity dwarf galaxies can be explained by the **photodissociation of CO**
  Madden et al. (2020)

Metallicity dependence of the CO-to-H_2 conversion factor

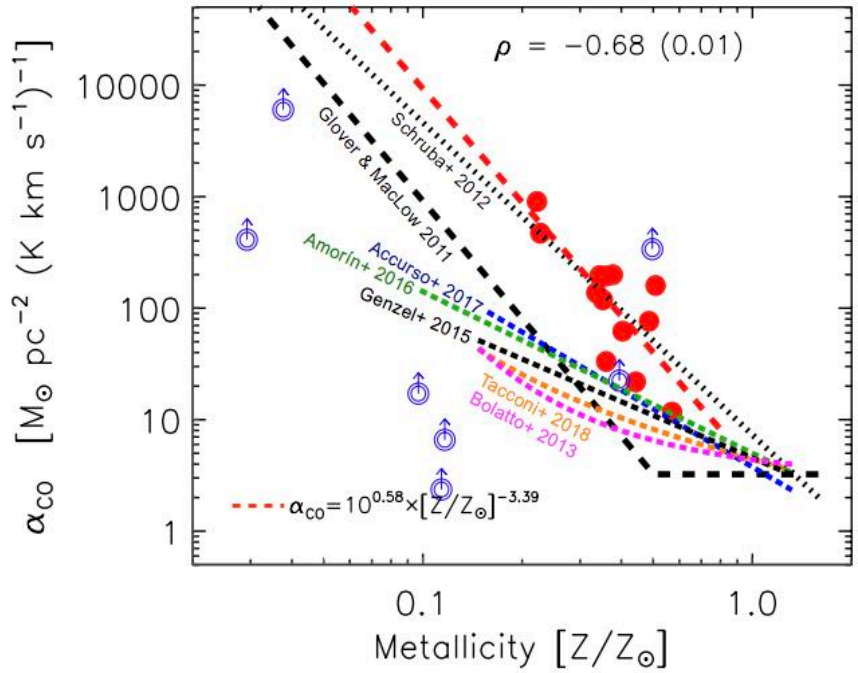

Madden et al. (2020)

- The low CO/SFR and high [C II]/CO observed in low metallicity dwarf galaxies can be explained by the **photodissociation of CO**
  Madden et al. (2020)
- The **UV photons leaking out** of young star-forming regions could be responsible for this photodissociation of CO

Metallicity dependence of the CO-to-H_2 conversion factor

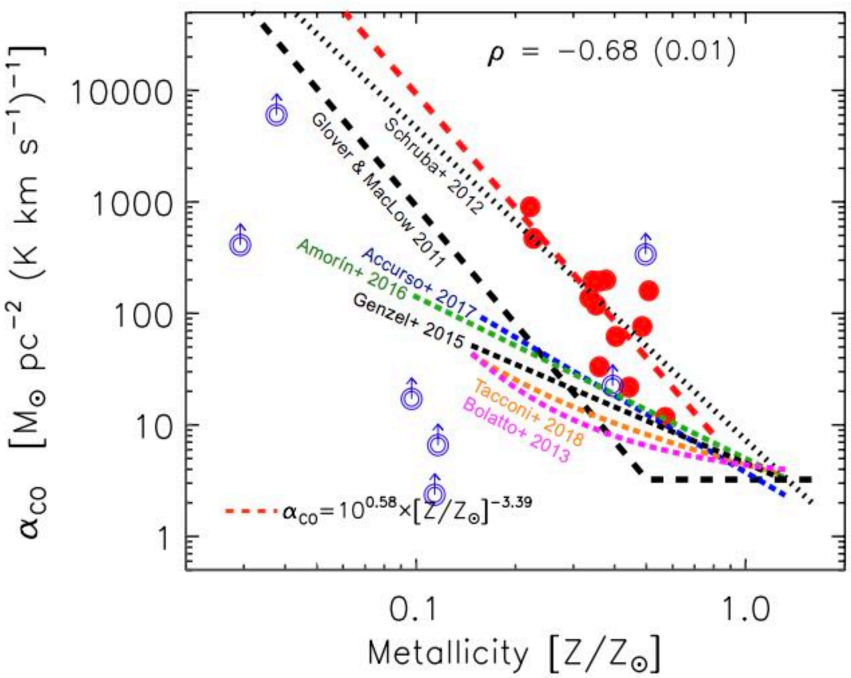

Madden et al. (2020)

- The low CO/SFR and high [C II]/CO observed in low metallicity dwarf galaxies can be explained by the **photodissociation of CO**
  Madden et al. (2020)
- The **UV photons leaking out** of young star-forming regions could be responsible for this photodissociation of CO
- This is increased at low-metallicity due to a **more porous ISM**
  Chevance et al. (in prep.)

Metallicity dependence of the CO-to-H_2 conversion factor

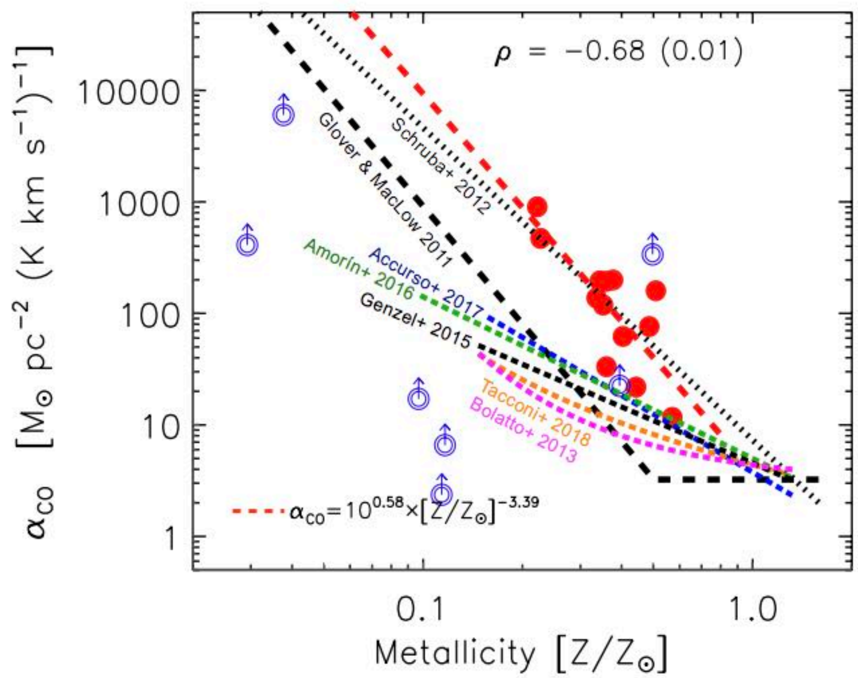

Madden et al. (2020)

- The low CO/SFR and high [C II]/CO observed in low metallicity dwarf galaxies can be explained by the **photodissociation of CO**
  Madden et al. (2020)
- The **UV photons leaking out** of young star-forming regions could be responsible for this photodissociation of CO
- This is increased at low-metallicity due to a **more porous ISM**
  Chevance et al. (in prep.)
- Results in the presence of a **large reservoir of CO-dark molecular gas**

Conclusions

- Using PDR modelling, FIR emission lines reveal the **3D structure** and the **physical properties** of the gas
- In massive star forming regions the vast majority of the molecular gas is **CO-dark**

Conclusions

- Using PDR modelling, FIR emission lines reveal the **3D structure** and the **physical properties** of the gas
- In massive star forming regions the vast majority of the molecular gas is **CO-dark**

This is driven by:

- The **intense radiation field** from the central cluster
- The **high porosity** of the gas in moderate to low-metallicity environments, allowing a **large fraction of the photons to escape** young stellar regions and travel over tens of parsecs
- Next step: bridging cloud-scale conditions to the **larger scale environment**

Future work

LMC+: SOFIA Joint Legacy Proposal proposal with FIFI-LS (C9) on the LMC Molecular Ridge *(P.I.: S. Madden and A. Krabbe)*

- **50h: 1.3x0.5 deg map in [CII] and [OIII]**

- physical conditions and thermal processes in the PDRs
- quantify the total molecular gas mass reservoir
- probe a wide variety of star-forming and ISM conditions

- complement the recent accepted ALMA proposal for CO observations of the ridge (PI: Bolatto)

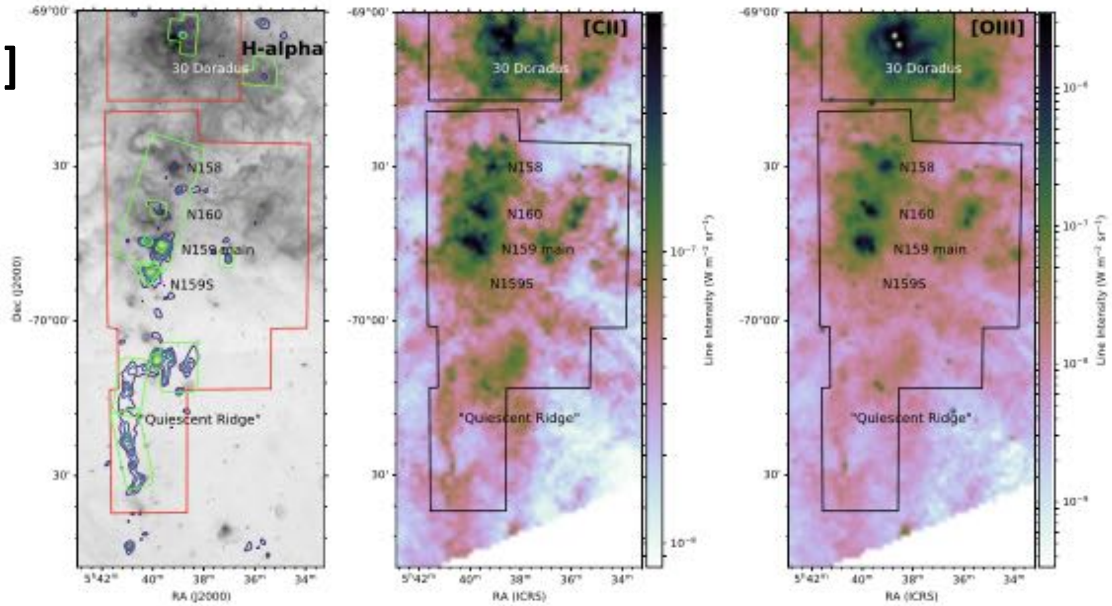

MCELS Hα
(Paredes et al. 2015)
CO contours
(MAGMA; Wong et al. 2011)

Simulated [CII] 158µm and [OIII] 88µm

Conclusions

- Using PDR modelling, FIR emission lines reveal the **3D structure** and the **physical properties** of the gas
- In massive star forming regions the vast majority of the molecular gas is **CO-dark**

This is driven by:

- The **intense radiation field** from the central cluster
- The **high porosity** of the gas in moderate to low-metallicity environments, allowing a **large fraction of the photons to escape** young stellar regions and travel over tens of parsecs
- Next step: bridging cloud-scale conditions to the **larger scale environment**